UNRESTRICTED.

Tandem Mass spectrometry of Polyketide Natural Products

By Gordon Christopher Kearney
BSc (Hons)

Submitted for the Degree of MPhil.

23rd June 2002

Submission date: 27 June 2002
Award date: 26 February 2003

ProQuest LLC.
789 East Eisenhower Parkway
P.O. Box 1346
Ann Arbor, MI 48106 – 1346

Abstract

The polyketides form a group of natural products, related biochemically to both fatty acids and non-ribosomal peptides, that contains many important antibiotic drugs.

The macrolide polyketide drugs, such as erythromycin, are biosynthesised on giant, modular enzymes. These may be manipulated genetically, leading to the production of novel analogues of the original compound. These analogues must be structurally characterised.

Tandem mass spectrometry (MS/MS) can provide a spectrum of characteristic fragment ions. The collision induced dissociation (CID) of protonated erythromycin A and *sec*-butylerythromycin B was investigated using MS/MS on an ion-trap mass spectrometer. In order to investigate the nature of the fragmentation processes that occurred the experiments were repeated, after substitution of exchangeable hydrogens for deuterium.

MS/MS experiments were also carried out on a quadrupole/time of flight (Q-Tof) mass spectrometer. Accurate-mass Q-Tof spectra allowed the assignment of elemental compositions to fragment ions. ^{18}O labelling of the C-9 carbonyl group gave insight into the first elimination of water from the parent ion.

In order to probe further the mechanisms of unimolecular dissociation for this class of molecule MS/MS experiments were carried out on roxithromycin and oleandomycin, two compounds similar to erythromycin. The C-9 oxime group of roxithromycin is eliminated in an analogous way to the C-9 carbonyl group of erythromycin A. Also, since oleandomycin has no C-6 hydroxyl group, macrolide ring opening reactions do not occur.

A scheme is tentatively proposed for the CID fragmentation reactions of erythromycin A.

Chapter 1

Introduction to Polyketide Natural Products

There are many, varied metabolic processes which occur in living organisms and these can be divided into two main categories. Primary metabolism includes the biosynthetic (anabolic) and degradative (catabolic) biochemical reactions that are essential to the survival of a cell or organism. Included in this category is the biosynthesis of proteins, lipids, carbohydrates and DNA together with such catabolic processes as the oxidation of sugars during glycolysis. Secondary metabolism is a term used to denote metabolic pathways that have no essential function, although secondary metabolites may play an important role in the life of an organism. Secondary metabolites that are unique to a species or a closely related group of species are known as natural products.[1]

One group of natural products, known as polyketides, is derived from acyl building blocks such as acetate, propionate, malonate and methylmalonate. The biosynthesis of polyketides is related to that of fatty acids and proceeds in a similar way. The process is catalysed on giant multifunctional polyketide synthase (PKS) enzymes that bring about a series of repeated carbon chain extension reactions, each of which extend the polyketide chain by a C_2 unit.

A type 1 or reduced polyketide may contain keto, hydroxyl, alkene and methylene functions at various positions in the polyketide chain. This, together with the fact that a range of starter and extender units may be incorporated, that chain length may be varied and that stereochemistry may be controlled makes the reduced polyketides a structurally diverse and important class of natural products (Figure 1.1).

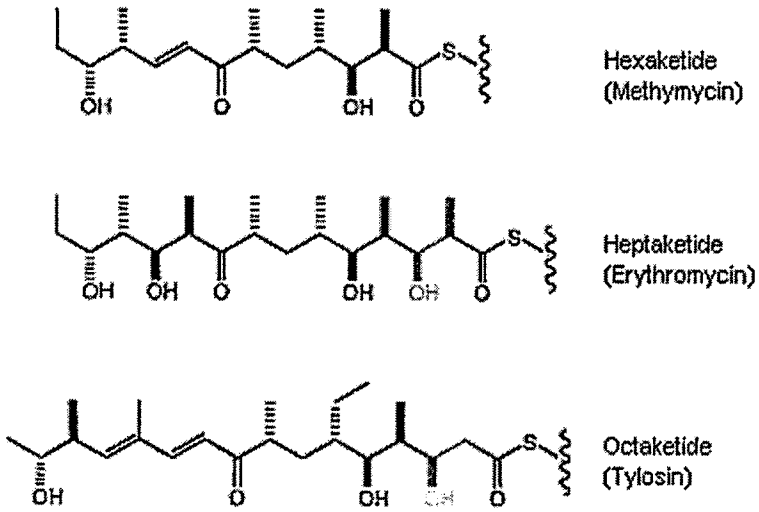

Figure 1.1

A type 1 PKS is arranged in a series of modules; each module serves to perform one C_2 unit extension together with a predetermined level of β-keto reduction. The polyketide chain is then passed to the next module, via thioester exchange, for further processing.

Each module consists of certain core domains. A β-ketoacyl synthase (KS) catalyses the decarboxylative condensation that gives chain extension, an acyl carrier protein (ACP) serves as a flexible arm for transporting the polyketide chain, thioester linked, to the various catalytic sites and an acyl transferase (AT) loads a starter or extender unit onto the ACP. These domains are essential for polyketide chain extension. The mechanism of Claisen-type decarboxylative condensation is shown for a methylmalonyl extension (Figure 1.2).

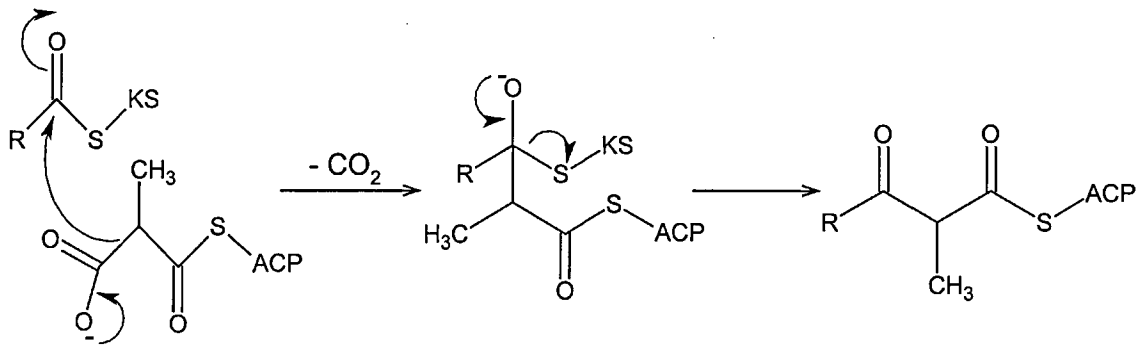

Figure 1.2

There are also three types of domain which catalyse the three stages of β-keto reduction. A β-ketoacyl reductase (KR) catalyses reduction of a β-keto group to a hydroxyl, an enoyl reductase (ER) catalyses dehydration of a hydroxyl group to an alkene, and a dehydratase (DH) catalyses reduction of an alkene group to methylene. The presence or absence of these domains determines the extent of reduction that occurs. A diagram of a chain extension module with a complete reductive loop is shown (Figure 1.3).

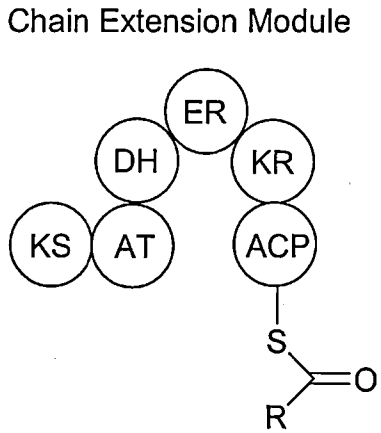

Figure 1.3

The sequence of events that occurs in a single chain extension step is as follows. The ACP from the module immediately upstream from the module in question loads the growing polyketide chain onto the KS. The AT loads an extender unit, such as malonate, onto the ACP (Figure 1.4).

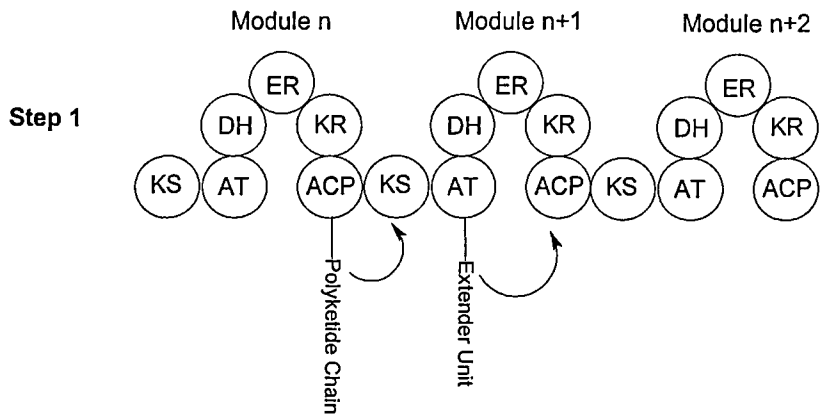

Figure 1.4

The ACP transfers the extender to the KS where decarboxylative condensation occurs and the polyketide is simultaneously extended and transferred to the ACP (Figure 1.5).

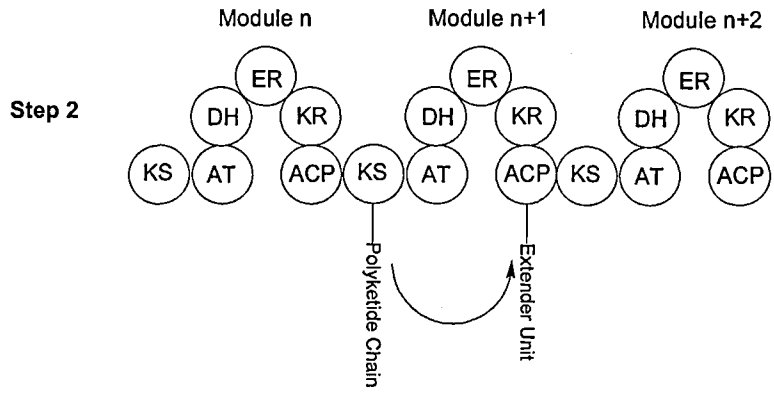

Figure 1.5

The newly extended polyketide chain is then transferred sequentially around any reductive domains present in the module (Figure 1.6).

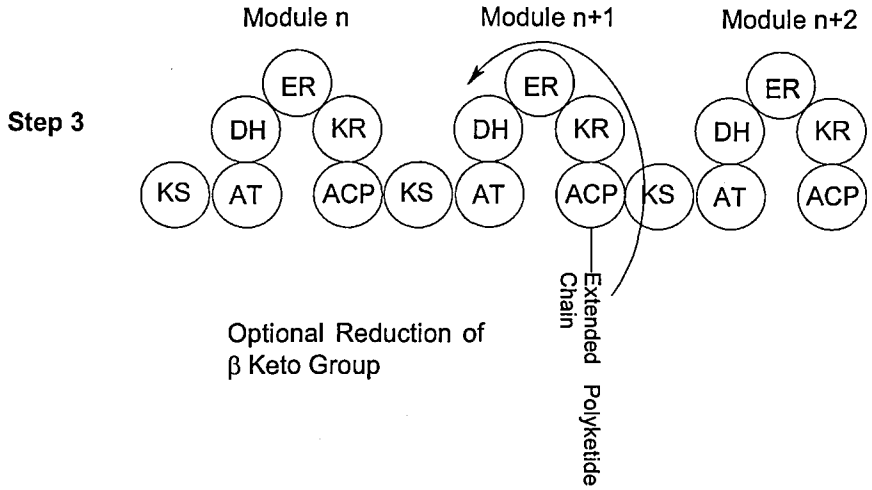

Figure 1.6

The processed chain is then transferred to the KS of the next module for further processing.

A final thioesterase (TE) domain catalyses the off-loading of the completed polyketide molecule by hydrolysis of the thioester bond. Once offloaded, polyketide molecules are often modified by a series of tailoring steps such as *O*-methylation, hydroxylation and glycosylation.[2, 3]

The macrolides are a group of polyketides characterised by their macrocyclic lactone rings. It is a clinically and commercially important group that includes antibiotics, immunosuppressants, antifungals and antitumor agents. There are two main types. One class contains molecules such as rapamycin (Figure 1.7a) that can be viewed as a polyketide-peptide hybrid. The other contains 12, 14 or 16-membered macrolides that have been

modified by the addition of sugar groups (glycosylation). Glycosylation is a very important step in the biosynthesis of macrolide antibiotics since the unmodified aglycone often displays no antibacterial activity. Common ancestry is evidenced by the fact that structural similarities exist between members of this group, as first observed by Celmer.[4]

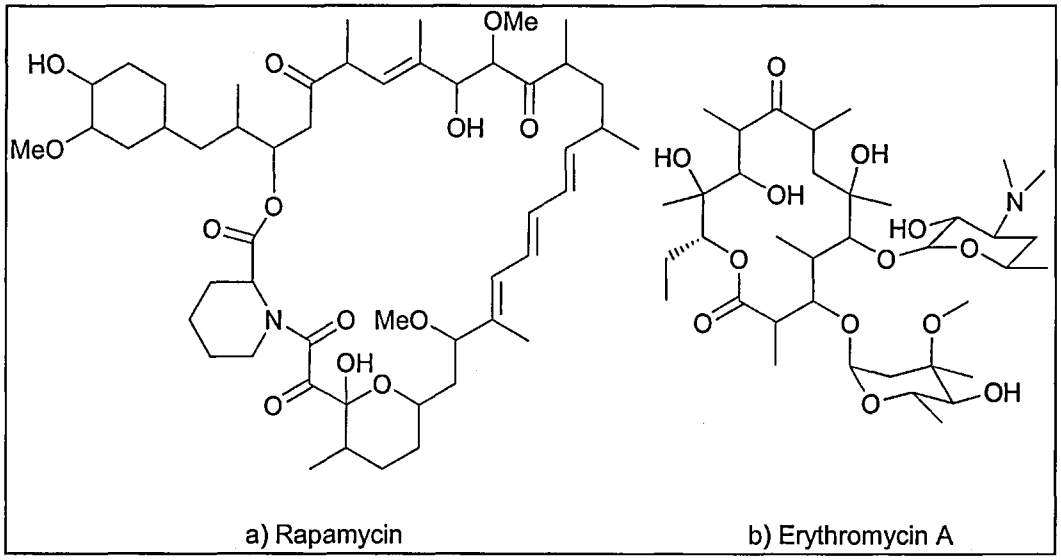

Figure 1.7

One of the most important families of macrolide antibiotics is the erythromycins. They contain a 14-membered ring and two sugar moieties, one at C-3 and one at C-5. Erythromycin A (EA) (Figure 1.7b), the first to be discovered, is an antibiotic active against Gram-positive bacteria. It was first isolated in 1952 from the soil bacterium *Saccharapolyspora erythrea*.[5] The first isolable intermediate in the biosynthesis of erythromycin is the unmodified aglycone 6-deoxyerythronolide B (6-dEB).[6] It is formed on the 6-deoxyerythronolide B synthase (DEBS) PKS from one unit of propionyl CoA (the starter unit) and six units of methylmalonyl CoA (extender units). A scheme showing the modular biosynthesis of 6-dEB on the DEBS PKS is shown (Figure 1.8).

The overall synthase consists of three huge individual peptides that exist as homodimers. These are called DEBS1, DEBS2 and DEBS3 and the term "cassette" has been used to describe them. The three cassettes each contain two chain extension modules and they are linked to form the overall DEBS PKS. DEBS1 contains the loading domain and DEBS3 contains the TE function. The linking of the three cassettes must be such that the extending polyketide chain is passed from one module to the next until it is offloaded by the terminal TE.

Upon cyclisation and off-loading by the TE a series of tailoring steps occurs. The first is a C-6 hydroxylation that is catalysed by eryF, a cytochrome P450 hydroxylase. This yields

erythronolide B (EB) which is then modified by a glycosyltransferase that attaches L-mycarose at the C-3 hydroxyl. A second glycosyltransferase adds the amino sugar D-desosamine at the C-5 hydroxyl to yield erythromycin D (ED), the first intermediate to show antibacterial activity. Then a second hydroxylation takes place at C-12, catalysed by eryK, another cytochrome P450 hydroxylase, to yield erythromycin C (EC). Alternatively ED may undergo *O*-methylation at the C-3″ hydroxyl of the mycarose sugar to form erythromycin B (EB). Finally either EB undergoes C-12 hydroxylation or EC undergoes C-3″ *O*-methylation to produce EA (Figure 1.9).[3]

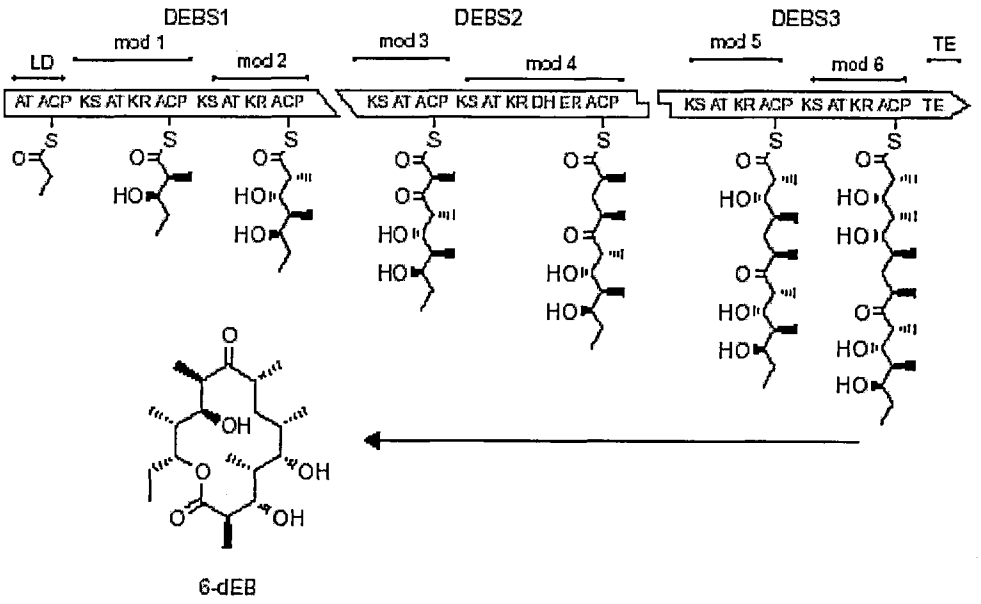

Figure 1.8

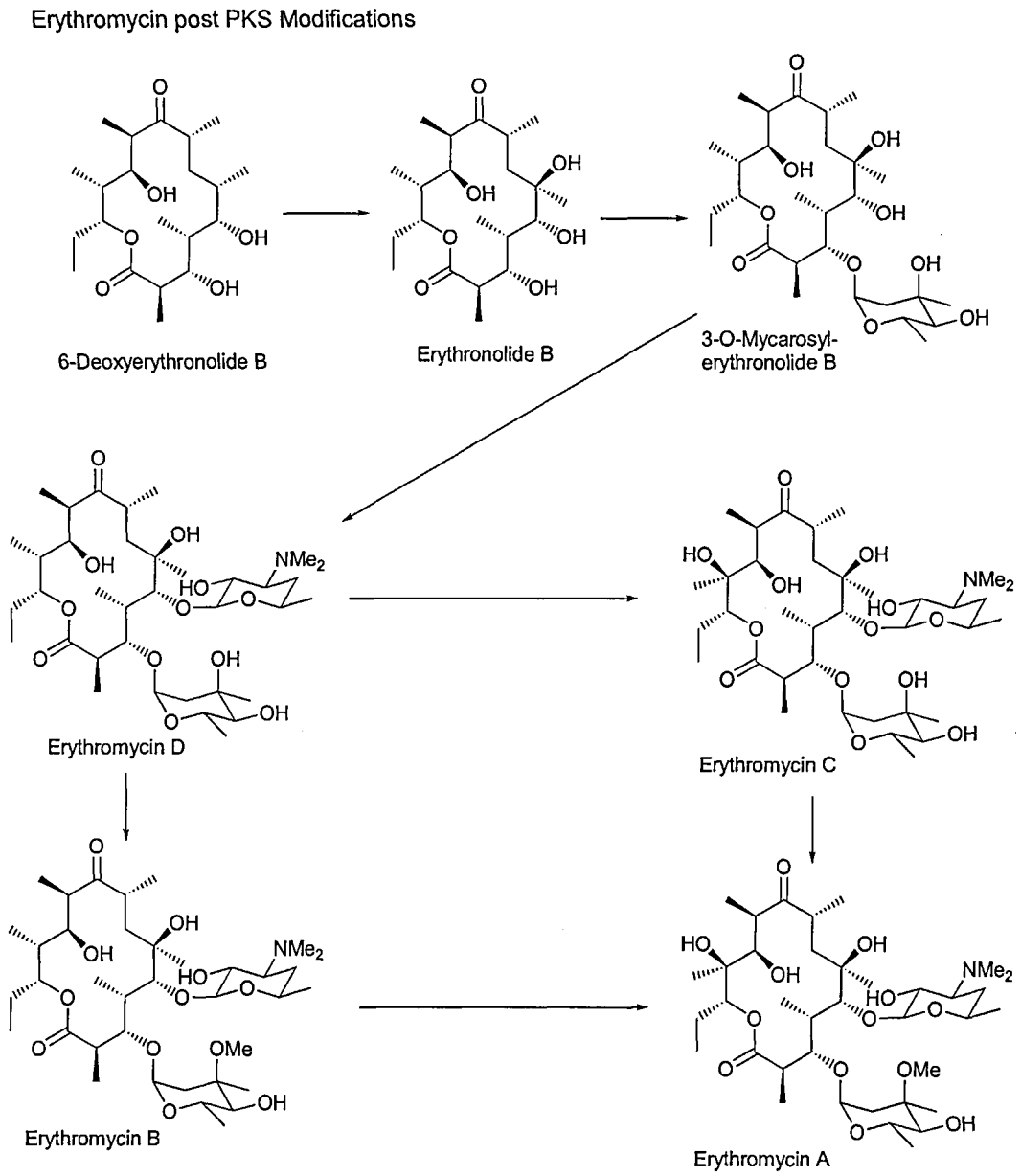

Figure 1.9

The modular nature of type 1 PKSs may be used to account for the diversity of structure along the polyketide chain. Each module and each domain within a module is able to catalyse a specific set of reactions. Stereochemistry and functionality of each polyketide extension is directly related to the type and specificity of domains present in a module. It has been shown by genetic engineering experiments, that it is possible to rationally alter modular polyketide biosynthesis in order to obtain a predicted novel analogue. This was first achieved by Katz and co-workers who inactivated the KR domain at module 5 in the DEBS PKS. The 5-keto analogue of mycarosyl-6-dEB was produced (Figure 1.10) demonstrating that natural PKSs may be manipulated to produce novel products.[7]

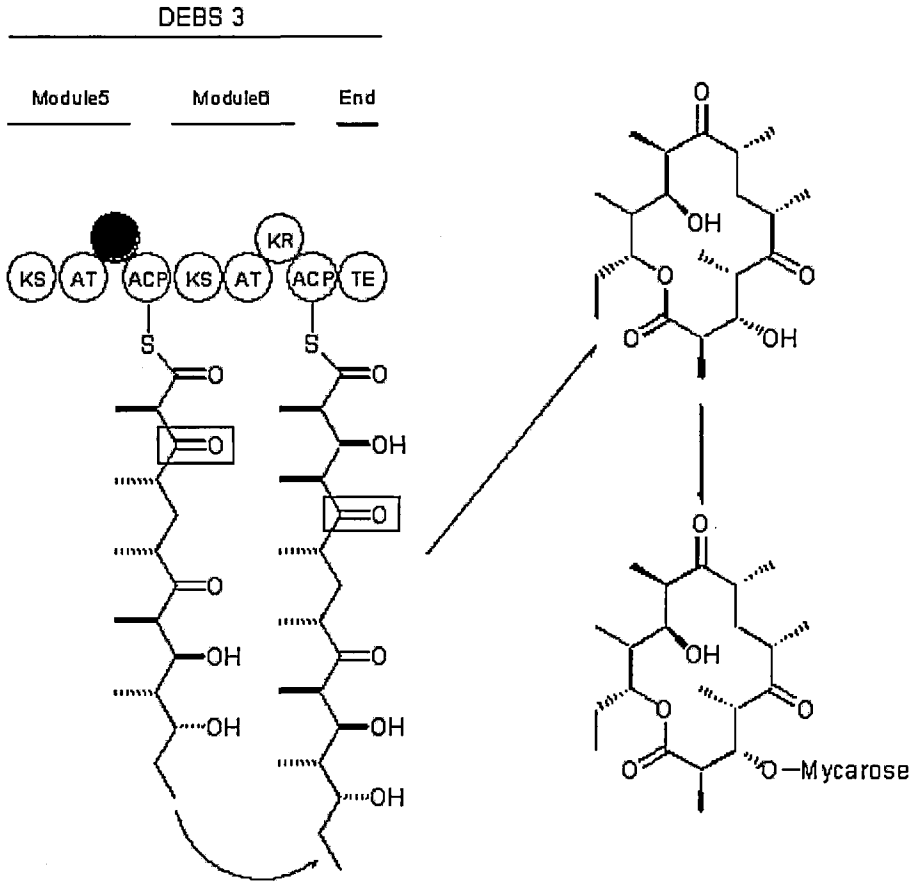

Figure 1.10

The next significant experiment in PKS engineering was conducted by Staunton, Leadlay and co-workers who demonstrated that a domain may be repositioned whilst retaining the ability to catalyse its normal type of reaction on a foreign substrate. The TE from Module 6 at the end of the DEBS PKS was repositioned at the end of module 2 (Figure 1.11). The truncated PKS system (DEBS 1-TE) produced no erythromycin but did produce the expected triketide δ-lactone.[8]

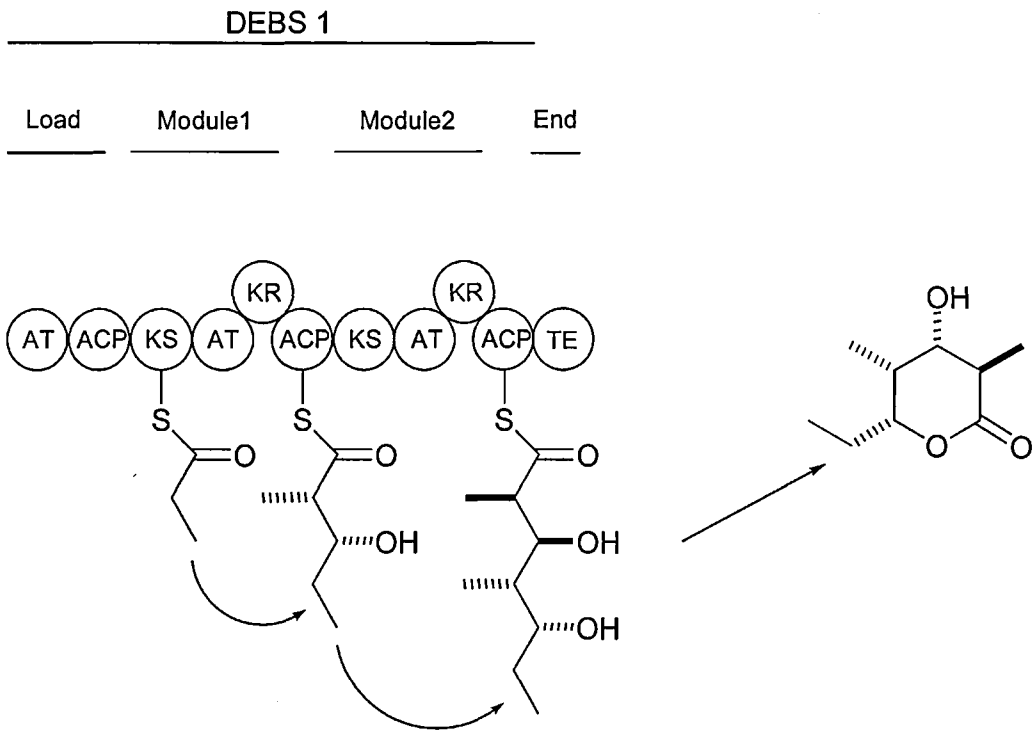

Figure 1.11

Since then further experiments have succeeded in engineering hybrid PKSs based on the DEBS system but incorporating domains or modules from other systems. For example, the AT from rapamycin module 2 specifically loads a malonyl extender group during normal rapamycin biosynthesis. When the DEBS 1-TE AT from module 1 (which loads a methylmalonyl extender) is replaced with this domain (shown shaded), the hybrid system produces the expected triketide δ-lactone lacking a methyl group at C-4 (Figure 1.12).[9]

Load Module1 Module2 End

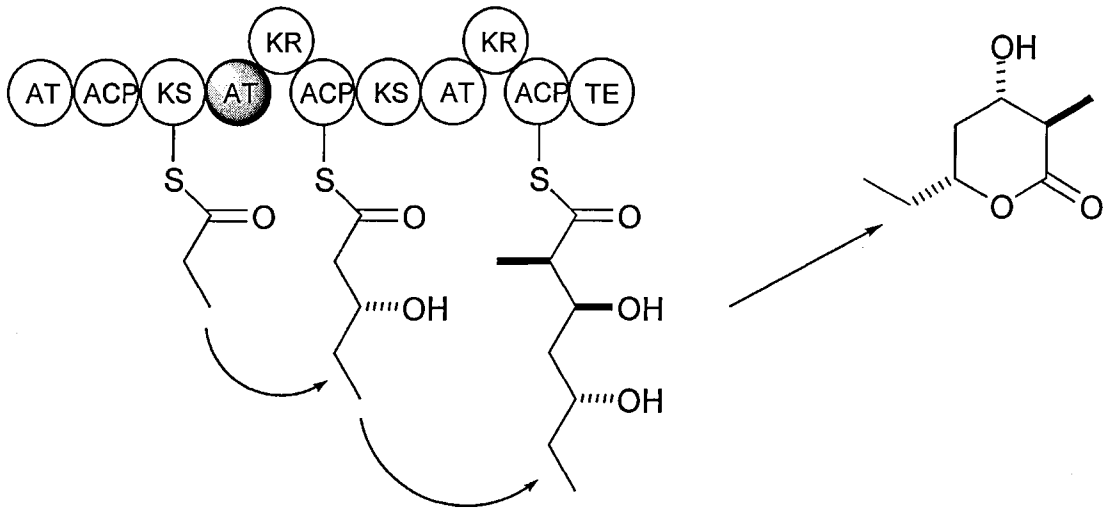

Figure 1.12

Another significant experiment involved replacing the DEBS 1-TE loading domain (which is specific for propionate starter but will accept some acetate) with that from the avermectin PKS. The avermectin loading domain has a relaxed specificity and will accept acetate, propionate, butyrate and *sec*-butyrate starter units. This novel PKS produced the four expected triketide δ-lactones.[10] This approach has been extended to the complete DEBS PKS where the avermectin loading domain has been able to incorporate exogenously fed acids to produce a variety of analogues of erythromycin each differing by the nature of the starter unit.[11] One difficulty with such a method is that administered acids must compete with the naturally occurring acetyl, propionyl and butyryl-CoA within the cell. A range of biosynthetic products may sometimes be seen.

A semisynthetic approach may be adopted in order to direct the biosynthesis of novel polyketide analogues. An inactivation of the KS1 of DEBS prevents the biosynthesis of 6-dEB. Synthetically derived diketide acids may then be fed as N-acetylcysteamine (NAC) thioesters. The NAC group mimics the phosphopantetheinyl group of the ACP, allowing loading of the diketide at module 2 of the PKS. The novel 6-dEB analogues may be generated with no competing side products.[12] A disadvantage of such a technique is the degree of effort involved in the synthesis of various diketide precursors.

Given the growing world-wide problem of pathogen resistance to commonly used antibiotics, such techniques offer the possibility that artificially altered polyketide

biosynthesis may generate lead compounds in the search for new antibiotic drugs. The ultimate goal of continuing experiments is the generation of combinatorial libraries of erythromycin analogues for pharmaceutical research.[13-17]

Significant advances have recently been made in probing the underlying mechanisms of polyketide biosynthesis. Since the PKS proteins are so large it has proved difficult to obtain structural information from techniques such as X-ray crystallography. One approach has been to investigate single catalytic domains. The DEBs TE was expressed in *Escherichia coli*, purified and crystallised. The structural information obtained from crystallography gave insights into the accurate orientation of the heptaketide chain when it is transferred to the TE. The chain is held in position by seven hydrogen bonds, whilst the C13 hydroxyl group is able to attack C1 to form the 14 membered ring.[18] Improved understanding of protein structure will ultimately allow a rational choice of TE for a given substrate when designing combinatorial, biosynthetic experiments.

Another recent advance has been the evolution of *E. coli* as a general host for the production of polyketides. Natural polyketide producing organisms, such as *Saccharapolyspora erythrea*, grow slowly and produce relatively small amounts of polyketide. *E. coli* is able to grow rapidly and can be made to produce large amounts of polyketide. Up to 180 mg/L of 6-dEB was produced in shake flask cultures.[19] Such rapid production of high yields should increase the rate at which combinatorial biosynthetic tools may be developed and used.

Such combinatorial biosynthetic experiments will present challenges to the analytical chemist charged with structural elucidation of the novel polyketide compounds. To fully characterise a molecule requires the growth of large quantities of bacterial culture followed by extraction and isolation of milligram quantities of analyte for techniques such as NMR spectroscopy. The large number of samples generated in combinatorial experiments may result in a bottleneck at the analytical stage. Analysis may be speeded up if more information could be obtained from preliminary HPLC tandem mass spectrometry (MS/MS) screening experiments conducted on small quantities of sample. A decision could then be made as to which fermentations require scaling up for further investigation.

The purpose of this study is to investigate the fragmentation reactions of polyketide macrolides under electrospray ionisation (ESI) and collision induced dissociation (CID). It is hoped that an understanding of such ion fragmentations will assist in the elucidation of the structure of novel polyketide natural products.

Chapter 2

Theory of Mass Spectrometry

Early History

Positively charged ions were first observed as luminous streamers passing through the perforations made in the cathode of an electrical discharge tube. They were deflected in electric and magnetic fields by Wien in 1898, who showed them to consist of positively charged particles.[20] This was followed in 1912 by the work of Thomson who developed an apparatus for the separation of positively charged particles in a magnetic field, according to their mass to charge ratio (m/z). His positive ray parabola instrument, the first mass spectrometer, for the first time proved the existence of an elemental isotope with the discovery of ^{22}Ne.[21] In 1919, Aston built the first velocity focusing deflection instrument. In Aston's instrument, a uniform electric field was placed before a magnetic field. Ions with varying kinetic energies were focused to a point by the electric field, prior to entering the magnetic field for mass analysis. The improved resolution obtained by this method allowed the isotopes of chlorine, mercury, nitrogen and the noble gases to be investigated.[22-24]

Dempster, in 1918, developed a different approach for the detection of ions deflected in a magnetic field. His mass spectrometer utilised a semicircular magnet. Unlike Thomson and Aston he did not use a photographic plate for the simultaneous detection of all the ions in a spectrum. Instead, by varying the accelerating voltage of the ions V, he showed that ions of different masses are sequentially brought into focus at a fixed detector. The m/z values may be calculated from the relationship $m/z = B^2r^2/2V$ where B is the magnetic field strength, r is the radius of the path traversed by the ions and V is the accelerating voltage applied to the ions.[25] This method, and a similar one where the value of B is varied over time, was eventually to supersede the photographic plate detection method of earlier instruments.

During the 1930s and 1940s ion optics began to be accurately calculated and instrument geometries steadily improved until, by the early 1950s, the first commercial instruments became available. This enabled scientists other than physicists to employ mass spectrometry as an analytical tool. At around a similar time the first experiments were being performed with other types of mass spectrometer, most notably the Time of Flight and Quadrupole Field instruments.[20] These, together with the later Paul Ion Trap and Ion Cyclotron Resonance instruments, have largely replaced Magnetic Sector instruments in many applications.

Ionisation Techniques

Mass spectrometry is the combination of two processes, sample ionisation followed by mass analysis and ion detection. A range of ionisation techniques has been developed in order to deal with a variety of sample types. The ones most commonly applied to the analysis of organic molecules are described.

Electron Impact and Chemical Ionisation

The electron impact (EI) source, perfected by Nier in the late 1940s, was applied to the ionisation of organic molecules.[26] The EI source (figure 2.1) operates in the following way. The electrons given off by a resistively heated rhenium filament (F) are accelerated across a potential difference of typically 70V towards an electron trap electrode (T). The electron beam passes through a region (I) which contains sample molecules in the vapour phase. Sample molecules are struck by electrons and are electronically, as well as vibrationally excited. Positive ions are formed when an electron is lost from a high-energy occupied molecular orbital, usually from a position of high electron density such as a lone pair on a heteroatom. An externally applied magnetic field is used to reduce the width of the electron beam resulting in a smaller energy spread of ions. A repeller plate (R) pushes the ions through collimating slits (A&B) and into an acceleration potential difference.

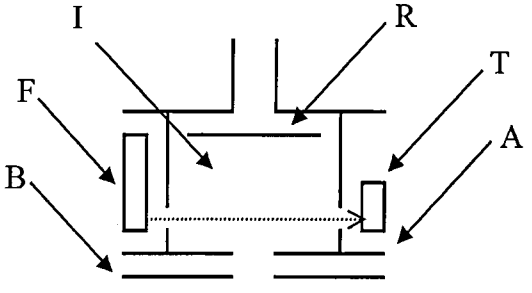

Figure 2.1

In the EI source, when an electron is lost from the sample molecule, radical molecular ions are formed. The energy transferred in this process usually causes some or all of the molecular ions to fragment in a manner characteristic of structure. Both heterolytic and homolytic bond fissions result in the generation of neutral molecules, neutral radicals, ions and radical ions with only a limited amount of rearrangement reactions taking place. An EI spectrum usually shows a high degree of fragmentation and there is sometimes no detectable amount of the molecular ion. Characteristic neutral losses can be readily identified and, from these, molecular structure may be inferred. For example, loss of 15 Da corresponds to a

methyl radical and loss of 17 Da to a hydroxyl radical. The amount of intramolecular rearrangement reactions that take place is limited because, for these to occur, specific molecular geometries are required and so their reaction rates tend to be lower than for single bond cleavages. An advantage of this method of ionisation is that a great variety of molecules will give useful spectra so long as they have a sufficiently high vapour pressure in the source region. A heated insertion probe and source block may be used to enable the vapourisation of some samples but, because of the involatility of large molecules, the useful mass range is limited to around 1000 Da. Polar molecules containing hydroxyl, amino or carboxylic groups are generally limited to a mass of around 300-400 Da.[27]

Another advantage of the EI source is that spectra obtained under standard conditions are comparable, regardless of the instrument used. This has enabled the compilation of vast databases of reference spectra that can be used to library match, and tentatively identify, an unknown spectrum.

One of the major disadvantages of EI ionisation is that there is often no molecular ion, so spectral interpretation is made more difficult. This problem may be overcome by the use of a less vigorous or 'softer', complementary technique known as chemical ionisation (CI).[28, 29]

CI is an alternative method of forming ions in the gas phase. The ionisation region (I) is flooded with a reagent gas such as methane or ammonia, at pressures approaching 1 Torr. The EI source is usually modified to contain this high pressure so that the gas is not immediately pumped away by the vacuum pumping system. The electron beam causes ionisation of the reagent gas and the reagent ions then cause secondary ionisation of the sample molecules, usually by transfer of a proton. The resulting mass spectrum often shows an intense pseudomolecular ion peak at MH^+ (or MNH_4^+ where ammonia is used as the reagent gas). This method yields molecular mass information and extends the usefulness of EI. Neither EI nor CI, however, is suitable for the analysis of large polar substances such as involatile salts, peptides or polysaccharides.

Fast Atom Bombardment and Fast Ion Bombardment

Two related techniques, known as Fast Atom Bombardment (FAB) and Fast Ion Bombardment (FIB), may be used for the analysis of polar or high molecular weight molecules.[30, 31] The useful mass range of these methods extends to over 10,000 Da. In both cases, the sample is mixed with a liquid matrix of low volatility, such as glycerol or thioglycerol, before being bombarded with heavy particles. In FAB, the bombarding particles are usually xenon or argon atoms whereas in FIB they are usually accelerated

caesium ions. The effect of bombardment is to overcome the intermolecular bonds in the surface layers of the sample-matrix mixture, causing ions to be ejected into the gas phase. FAB and FIB mass spectra usually contain abundant pseudomolecular ions such as MH^+, MNa^+ and MK^+ together with a sizeable quantity of fragment peaks. Often negative ion spectra may also be obtained.

Electrospray Ionisation

Electrospray is a term used to describe the creation of fine aerosols by the electrostatic dispersion of a liquid. It is a technique used in a variety of industrial applications, for example, the spray painting of car bodies and the application of pesticide formulations to arable crops. In the electrospray ionisation (ESI) source evaporation of charged aerosol droplets leads to the production of gas phase ions that may be analysed by mass spectrometry. A diagram of a typical Finnigan Corporation electrospray source is shown (Figure 2.2). The spray needle is held at a potential of around 3.5 to 4 KV and the solvent nebulisation process is assisted by the application of a co-axial nitrogen gas flow. The heated capillary causes the desolvation of the electrosprayed droplets and the tube lens focuses ions through the skimmer cone into the first vacuum region of the mass spectrometer.

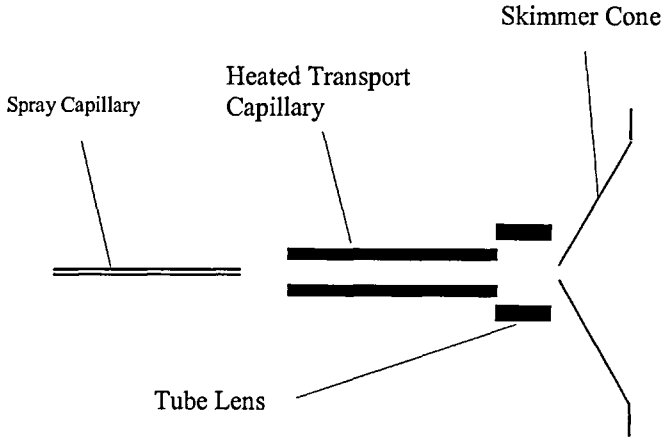

Figure 2.2

As early as 1968, ESI was used to generate gas phase ions of polystyrene with a weight-averaged molecular weight of 51,000 Da.[32,33] The production of these stable macroions was the first indication that ESI was one of the softest ionisation methods available. Softness is taken to mean the degree to which the molecular ion remains unfragmented by the ionisation process. In 1983 an ESI source was, for the first time, coupled to a conventional mass spectrometer and used for the study of ions below 450 Da.[34,35] The technique has now

become widely adopted for the mass spectrometric determination of both low and high molecular weight analytes. ESI ionisation is routinely applied to the analysis of large molecules such as proteins, polysaccharides and synthetic polymers.[36, 37] A unique feature in the ESI spectra of macromolecules is the phenomenon of multiple charging. For example, protein molecules may appear in the mass spectrum as a series of multiply charged molecular ions of low m/z value. The spectrum may be deconvoluted to yield an accurate measure of molecular mass.[38]

There are two theories of the mechanism of ESI ion formation. One is the Iribarne-Thomson ion-evaporation model. The other is the charge-residue model first proposed by Dole. Both models agree as to the initial stages of the ESI process in which solvent evaporates from charged droplets, which consequently reduce in size. The size reduction causes an increase in charge density at the droplet surface until the Rayleigh stability limit is reached, after which the droplet undergoes Coulombic fission to yield a number of smaller droplets. The Rayleigh limit is the point at which electrostatic repulsion becomes equal to surface tension. The smaller droplets continue to shrink until Coulombic fission occurs again. The process may be repeated several times.[39]

The charge-residue model proposes that, if the electrosprayed solution is dilute enough, then eventually some charged droplets are formed which contain just one solute molecule.[32] Upon evaporation of the remaining solvent a gas phase ion will be created. The Iribarne-Thomson model is a more complex explanation of the final processes of ESI ion formation. It proposes that when the charged electrospray droplets reach a small enough size spontaneous ejection of ions into the gas phase occurs and this process significantly competes with Coulombic fission when the droplet size is less than 10 nm in diameter.[40, 41] For very small droplets in the final stages of the ESI process it becomes difficult to distinguish between the two theories and the exact nature of the processes involved is unknown.[42]

Mass Analysis

Ions created in the processes outlined above may be analysed according to their mass to charge ratio by any of the following techniques. Before proceeding it is necessary to define the following terms.

- Resolution. This is the ability of the instrument to detect masses as separate peaks and is defined as the width of a peak divided by its mass. Two definitions of resolution are generally used. The first is the 10% valley definition that takes the peak width at 10% of the peak height. The other is the Full Width Half Maximum (FWHM) definition that takes peak width at 50% of the peak height. Resolution is usually quoted in FWHM figures for time of flight (TOF) instruments.

- Tandem Mass Spectrometry (MS/MS). This is a process in which a collision cell filled with an inert gas separates two mass spectrometers. The first mass spectrometer (MS1) is used to select a precursor ion of a particular m/z, which is directed into the collision cell. The precursor ions are fragmented by Collisionally Induced Dissociation (CID) and the product ions are analysed by the second mass spectrometer (MS2) in order to produce an MS/MS spectrum.

Magnetic Sector

This is probably the most familiar form of mass analysis. Ions are accelerated into a magnetic field where they are deflected as outlined at the start of the chapter. Modern instruments achieve high mass-resolution by the use of an electrostatic sector in series with the magnetic sector. The electrostatic sector is usually placed before the magnet although 'reverse geometry' instruments are sometimes used for the analysis of the kinetic energies of metastable ions. The kinetic energy of an ion is related to the geometry of the electrostatic sector by the following equation $mv^2/2=EeR/(2d)$. E is the voltage between two electrostatic plates, d is the distance between them, R is the radius of the path of the ion and m and v are the mass and velocity of the ion. Thus the radius of the path of an ion in the electric field is directly related to its kinetic energy, therefore only ions with the required kinetic energy will be focused at the entrance to the magnetic sector.[43] This allows resolutions of over 100,000 (10% valley) to be achieved. Magnetic sector mass analysers can been interfaced to any type of ionisation source and the high resolution spectrum that can be obtained assists in the determination of the accurate mass of an ion. The accurate mass of an ion may be used to determine its elemental composition.[20] Magnetic sector instruments are large and expensive and they have a slow scanning rate making them unsuitable for routine, undemanding applications such as quantitative GC/MS analysis.

Quadrupole Field

The quadrupole mass analyser is, by contrast, small, light and inexpensive with a relatively fast scanning rate. It is not possible to obtain high-resolution data from an instrument of

this type but where such information is not required, the quadrupole mass spectrometer is often the instrument of choice. Bench-top instruments exist which are capable of performing MS/MS experiments. To perform MS/MS experiments using magnetic sector instruments involves doubling the size and complexity of the mass spectrometer since two instruments must be placed in series. The same is true of quadrupole instruments but the cost of placing two quadrupole mass analysers in series is considerably lower. For this reason magnetic sector instruments capable of performing MS/MS analyses are rare whereas quadrupole MS/MS instruments are very common. A quadrupole mass analyser consists of four parallel cylindrical rods that are electrically connected in pairs (Figure 2.3). Ions enter the space between the rods and drift parallel to them through the centre of the device. A DC voltage is applied across the rods in opposite pairs giving a two dimensional electric field in which ions will be repelled away from one pair of electrodes and towards the other. An ion located in the centre will be at zero potential with respect to the rods. An RF potential is superimposed over the DC potential. Lower mass ions are moved by the RF component more easily than higher mass ones. In the xz plane the DC component produces focusing but when a large enough RF voltage is applied, lower mass ions become unstable in the x direction. In the yz plane the DC field is defocusing but the RF voltage counteracts this effect for low mass ions, allowing only high mass ions to be lost in the y direction. Only ions with the required mass to charge ratio will have stable trajectories in both the x and y directions; all other ions will be filtered out. The mass spectrum is scanned by varying the RF and DC voltages whilst keeping a constant ratio between the two. By changing the ratio of RF to DC voltage the resolution of the instrument may be varied.[20, 44, 45] Whereas resolution in sector instruments is a constant value over the mass range (so that lower mass peaks are more separated than higher mass ones), quadrupole instruments maintain a constant level of mass differentiation and resolution varies over the mass range. Mass differentiation is usually set to 1 Da so that at a mass of 200, resolution is 200 (10% valley) and at a mass of 2000, resolution is 2000 (10% valley). Quadrupole instruments usually have an upper mass limit of about 4000 Da.

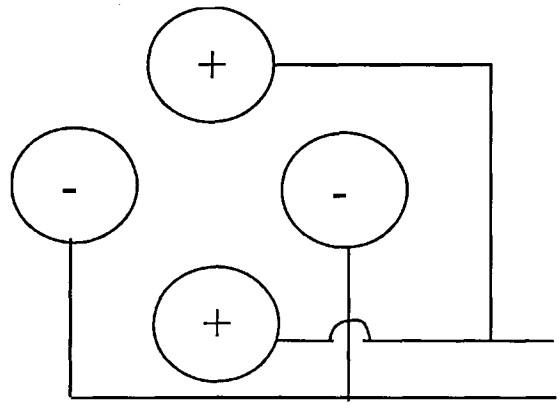

Figure 2.3

Time of Flight

The time of flight (TOF) mass spectrometer operates on a very simple principle. Ions are accelerated across a potential difference and into a drift tube (Figure 2.4). The kinetic energy an ion attains is related to its m/z ratio. The time an ion spends in travelling to the detector is related to its kinetic energy and so the travelling time is a measure of m/z value.[46,47] The basic relationship is $\sqrt{m/z} = A+Bt$ where A is an offset arising from delays in the timing electronics, B is a gain related to the dimensions and electric field strengths of the instrument and t is the flight time of an ion. TOF instruments are most readily coupled to pulsed ionisation sources such as laser desorption, where all the ions created in a discrete ionisation event can be sampled. Ionisation methods that produce a continuous supply of ions are usually coupled in an orthogonal geometry, so that the direction of travel along the drift tube is at right angles to the direction of ion extraction from the source. This ensures that the spread of kinetic energies of the sampled ions is small in the z direction allowing for higher mass resolution in the spectrum. Resolution is further increased by the use of an electrostatic mirror, or reflectron, at the end of the drift tube. This reflects and velocity focuses the ions, so that they arrive at the detector in more sharply defined bunches. It also doubles the length of the path that the ions travel and this also increases resolution between peaks.[48] Modern commercial instruments can easily achieve resolutions of around 20,000 (FWHM). The main benefits of a TOF mass analyser include the fact that it has a theoretically unlimited mass range and that it has the ability to sample a greater proportion of the ions produced in an ion source, since it is not a scanning instrument. The previous two types of instruments scan across a mass range so that at any given time, only ions of a particular mass to charge ratio are focused at the detector. This means that the overall sensitivity of the instrument is reduced except in certain applications where a single mass

may be continuously monitored. A TOF mass spectrometer rapidly samples all ions simultaneously and is much more sensitive than a scanning instrument in the full scan mode.

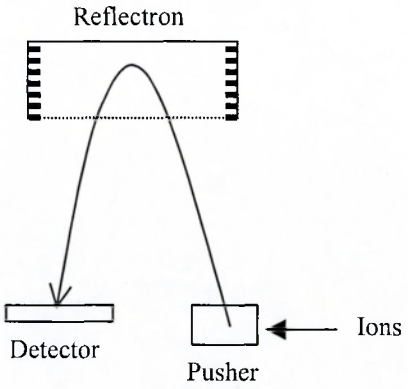

Figure 2.4

Quadrupole (Paul) Ion Trap

The Paul or quadrupole ion trap (QIT) (Figure 2.5) was first described in 1953.[44] Finnigan Corporation introduced the first commercial QIT mass spectrometer in 1983 and since then QIT mass analysers have been coupled to most types of ion sources.

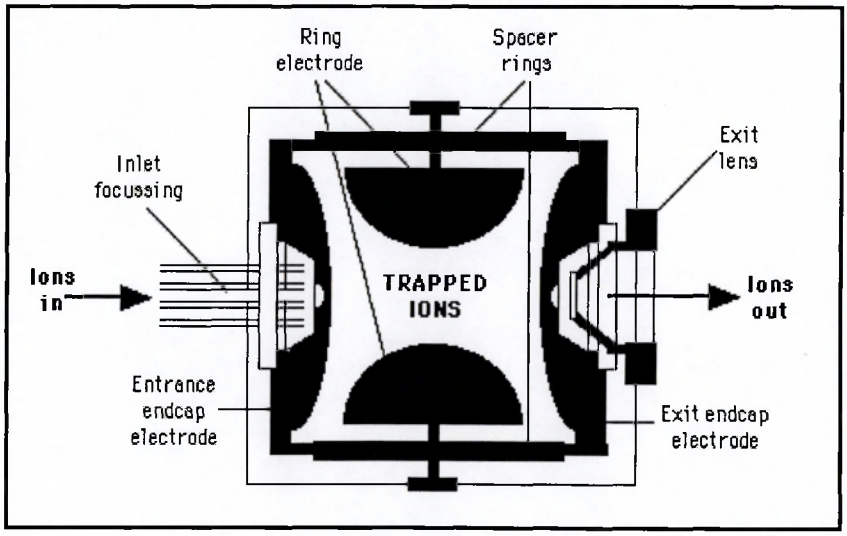

Figure 2.5

The device consists of three electrodes arranged to give a three dimensional electric field when suitable voltages are applied. A DC voltage is applied between the end-cap and ring electrodes and a trapping RF voltage is applied to the ring electrode. The QIT can be visualised as follows. If one pair of rods of a quadrupole mass spectrometer was modified to form a ring electrode and the other pair was modified to form two end-cap electrodes then

ions would be trapped by the resulting three dimensional field. Instead of following a path along an axis parallel to four rods, ions would be forced back towards the centre of the trap.

Ions are injected into and ejected from the QIT via small holes machined into the centre of the ring electrodes. As the RF amplitude is increased, trapped ions of increasing m/z values are ejected from the device. They are detected as they leave the trap and a mass spectrum is generated. Helium buffer gas is maintained at a pressure of around 10^{-3} Torr within the trap so that collisions between helium atoms and trapped ions results in kinetic cooling of the ions. This kinetic cooling has the effect of bunching the ions at the centre of the trap so that the mass spectrum is more highly resolved.[49-51]

Because the ions are cooled to the centre of the trap, the electric fields generated by the motions of the ions can cause space-charge effects to occur. These effects result in a distorted mass spectrum so the ion density within the trap must be controlled. This is achieved by a process known as automatic gain control (AGC). Before each scan occurs a rapid prescan is performed in which the total ion current is measured. The value of this measurement determines the length of time that ions are injected into the trap. A high prescan ion current results in a shorter ion injection time. This allows the trap to be optimally filled so that both sensitivity and spectral integrity are achieved.[52] The advent of AGC allowed the QIT to operate as a commercially viable mass spectrometer, able to compete with the more established quadrupole instruments in, for example, GC/MS quantification applications.

The QIT is capable of MS/MS experiments without the need for two mass spectrometers to be placed in series. Selected masses can be stored in the trap whilst all others are ejected. The trapped ions are excited by a "tickle" AC voltage applied across the end caps and their motions increase in amplitude. They collide with the helium buffer gas and CID occurs. The product ion spectrum may then be obtained with a normal scan across the desired mass range.[53, 54] An advantage of this technique is that MS^n experiments may be performed (where $1 \leq n \leq 10$).[55, 56] This allows the genealogy of a fragment ion to be determined. A disadvantage is that only limited amounts of energy may be imparted to the ion since too great a tickle voltage pushes the ions out of the trap.[57] Another disadvantage is that low mass ions are not stored during the CID stage of the MS/MS experiment. The cut-off point is at approximately 1/3 the mass of the precursor ion. This means that for a molecular ion of m/z 734 the lowest mass that can be seen in the MS/MS spectrum is at around m/z 240.

Fourier Transform-Ion Cyclotron Resonance (Penning) Ion Trap

In a homogenous magnetic field ions describe circular paths with a frequency which is independent of velocity but which is linearly dependant on mass. This frequency is given by the formula $\omega_c = Bz/m$ (where B is the magnet field strength, z is the charge and m is the mass of the ion), and is termed the cyclotron frequency.[58] In a Fourier transform-ion cyclotron resonance (FT-ICR) instrument the cyclotron motions of the trapped ions are excited by the application of a range of frequencies corresponding to the mass range of interest. The ions continue in their excited orbits until some loss of energy occurs upon collision with residual gas. The signal generated by the decay of ions to their original orbits is recorded and converted to a mass spectrum by Fourier transformation.[59] The technique is non-destructive and trapped ions may be repeatedly analysed and the signals averaged in order to improve signal to noise ratios. With high field superconducting magnets very high resolution can be achieved (over 1,000,000 10% valley), although resolution is inversely proportional to mass. One important feature of an FT-ICR mass spectrometer is the ability to perform high resolution, accurate mass, MS^n experiments on isolated precursor ions.[60]

Chapter 3

Fragmentation Mechanisms of Even Electron Organic Ions

Molecules are fragmented as a result of the energy imparted to them during processes such as EI ionisation, and a series of fragment ions is generated. These can be used to determine aspects of the structure of the parent molecule.

Techniques such as ESI and FAB ionisation are often used for the analysis of large, polyfunctional molecules such as peptides, natural products and polymers. The spectra produced from such molecules, and in some cases mixtures of molecules, can be difficult to interpret because of their complexity. These softer ionisation methods can usually generate a quantity of structurally diagnostic fragment ions but the mass spectrum is complicated by the molecular adducts that are often formed. For example, with ESI and FAB ionisation the mass spectrum may contain protonated, ammoniated, sodiated and potassiated molecular adducts together with dimers and higher order multimers. Sometimes multiply charged species are seen. All of these pseudomolecular ionic species may fragment and it is often difficult to determine which precursor ion gives rise to a given fragment ion. This sometimes limits the ability to decipher ESI and FAB spectra.

Two mass spectrometry experiments may be conducted in series so that the first stage of mass spectrometry (MS1) is used to select a predetermined m/z value. Ions at this m/z value are accelerated into a chamber containing an inert gas. Collisions between the ions and the gas cause collisionally induced dissociation (CID) to occur. CID takes place when collisions with the gas generate a population of ions in various vibrational and rotational excited states. As a result a range of unimolecular dissociations can occur that give rise to a series of fragment ions. The relative abundance of each of the fragment ions depends on the activation energy of the fragmentation reaction, the rate of the fragmentation reaction, the time available for reaction, the potential difference over which the ions are accelerated into the collision chamber and the nature and pressure of the collision gas.

The product ions may then be analysed using a second stage of mass spectrometry (MS2) and the procedure is known as tandem mass spectrometry (MS/MS). MS/MS experiments allow the correlation of a fragment ion with its parent.

Fragmentation reactions can occur in both odd electron (radical ion) and even electron ions. The radical ions that are usually generated by EI ionisation have been extensively studied.[27, 61] The softer ionisation processes such as ESI and FAB however, usually generate even

electron ions and, in the case of ESI, very little fragmentation occurs spontaneously. In order to obtain a structurally diagnostic fragmentation spectrum of such ions, some form of MS/MS experiment is necessary. This chapter has been limited to a discussion of the fragmentation mechanisms of even electron ions under CID conditions, since these reactions are of most relevance to this study.

With radical ions, homolytic bond cleavages often occur with the generation of an even electron ion and a neutral radical. In even electron ions such cleavages would result in the energetically unfavourable generation of a radical ion with a neutral radical. Even electron ions, therefore, generally fragment by heterolytic bond cleavages.[62] However, under high energy (KeV collision energy) CID conditions, such as those possible in magnetic sector instruments, homolytic bond cleavages can occur. In 1992 Maleknia and Brodbelt proposed mechanisms for the high energy CID fragmentations of crown ether-alkali metal ion adducts. They used a sector tandem mass spectrometer in $E_1B_1E_2B_2$ (E corresponds to an electrostatic and B to a magnetic analyser) configuration with a collision energy of 7KeV. Helium collision gas was maintained at a pressure low enough to give single collision conditions. The fragmentation mechanisms proposed involved a combination of homolytic carbon-carbon bond cleavages together with hydride rearrangement to give a series of distonic radical product ions (Figure 3.1).[63]

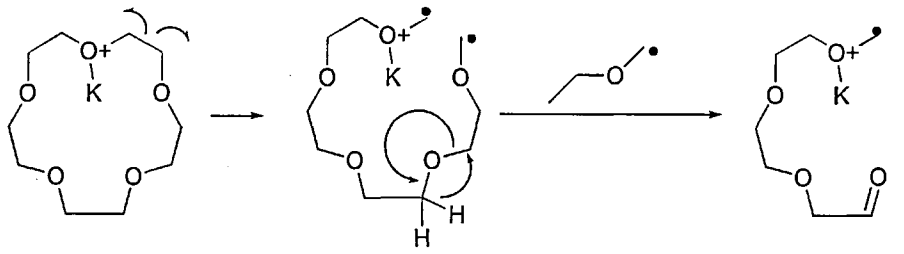

Figure 3.1

Under the low energy CID conditions usually found in ion traps and quadrupole instruments, fragmentation mechanisms involve the migration of pairs of electrons. The mechanisms can be classified as those that are charge driven or as charge remote. Charge remote fragmentation reactions are those where the site of reaction is distant from, and not directly driven by the location of charge. An example of this type of fragmentation mechanism is the high energy CID of fatty acids. For this class of molecule FAB ionisation has been used to produce both $[M - H]^-$ and $[M - H + 2Li]^+$ pseudomolecular ions, and CID fragmentation of these ions results in a series of losses corresponding to C_nH_{2n+2}. The mass peaks in the MS/MS spectrum appear at intervals of m/z 14. These same neutral losses are

observed regardless of the polarity of charge on the precursor ion and the proposed mechanism is a 1,4-H_2 elimination (Figure 3.2).[64-66]

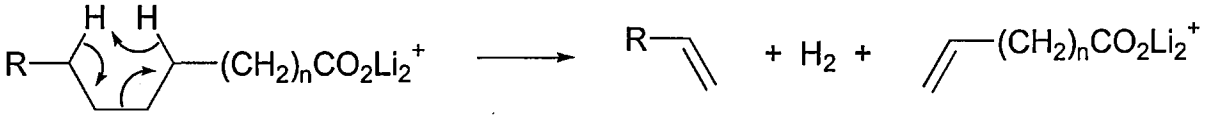

Figure 3.2

Charge remote fragmentations of this type require high energy CID conditions but other types can be low energy processes. An example of a low energy charge remote fragmentation is the loss of a sugar group that can occur in the CID of polyketide macrolide antibiotics. A hydride transfer process results in the formation of a carbon-carbon double bond in the sugar group and the generation of a hydroxyl group on the macrolide ring (Figure 3.3).[67]

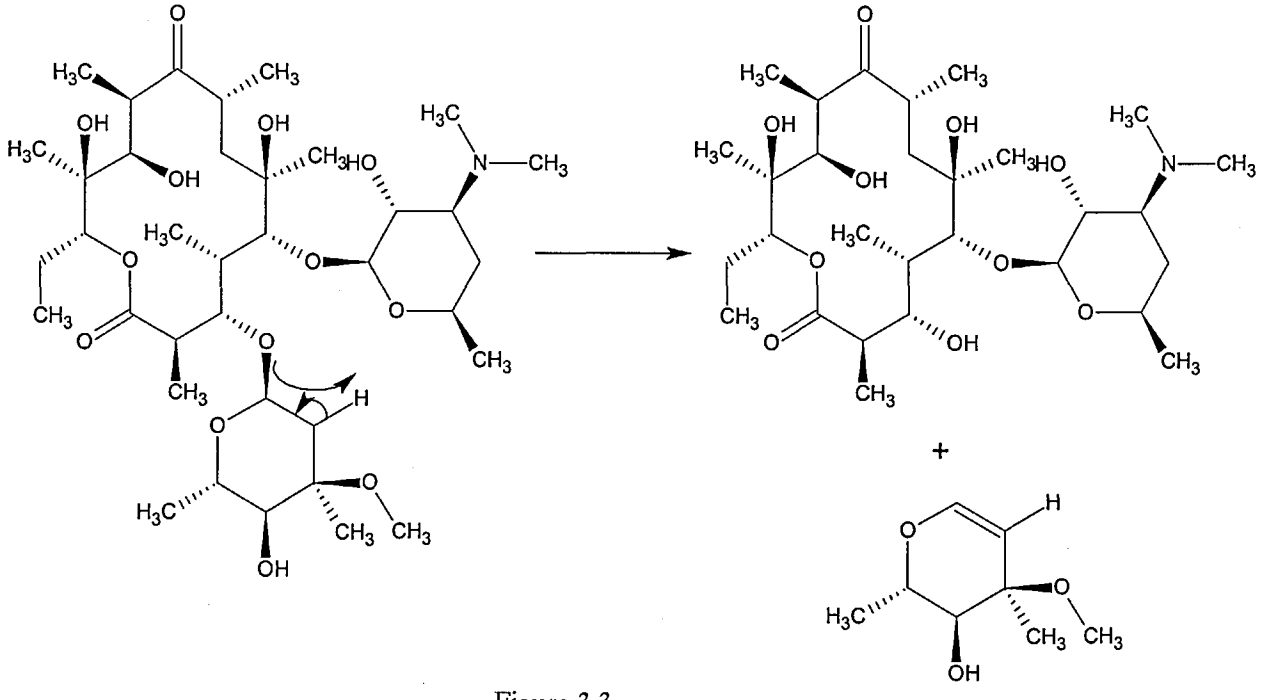

Figure 3.3

As a general rule, when an odd number of heterolytic bond cleavages occur, the atom that originally bore the charge is lost as part of the neutral fragment. Where an even number of bond cleavages occur, the atom that originally bore the charge is retained in the product ion. An odd number of bond cleavages must, therefore, result in charge migration reactions (e.g. Figure 3.4).[68]

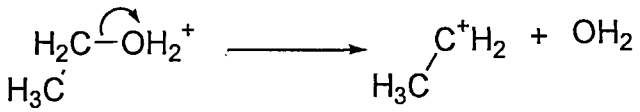

Figure 3.4

Even numbers of bond cleavages can result in charge retention reactions (e.g. Figure 3.5).[69]

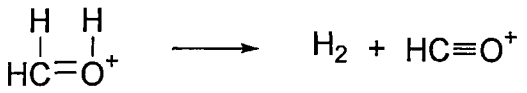

Figure 3.5

For many fragmentation reactions to occur some form of preliminary rearrangement is often required. Such rearrangements are common in the low energy CID of organic molecules and they sometimes serve to complicate the interpretation of MS/MS spectra. For example, when dimethyl ether was used as a CI reagent gas for the ionisation of phenol an ion was obtained which, upon CID in a quadrupole ion trap, undergoes a loss of 28Da. It was proposed that this corresponds to the elimination of a molecule of CO. The proposed mechanism for the loss proceeds via a migration of a methylene group to form a seven membered ring, hydride migration and finally a ring contraction to expel the CO (Figure 3.6).[70]

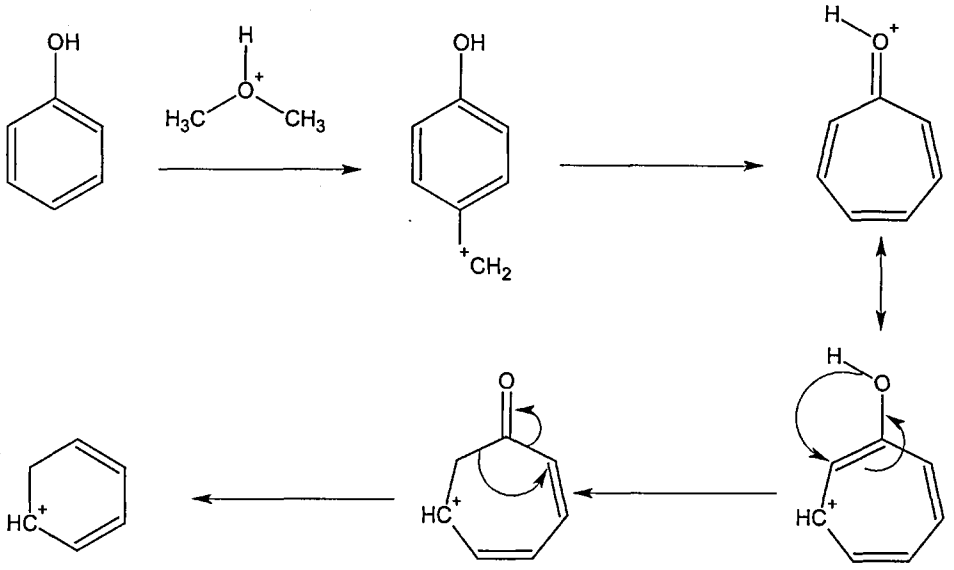

Figure 3.6

Even for such a relatively small molecule the mechanism of dissociation can be elaborate and complicated. For this reason isotopic labelling studies are sometimes used in order to investigate the processes involved.

Isotope labelling has been applied in order to discover the mechanism of the fragmentation of a polyamine spider toxin molecule. Two mechanisms were postulated for the generation of a fragment ion with a mass of 89Da (Figure 3.7).

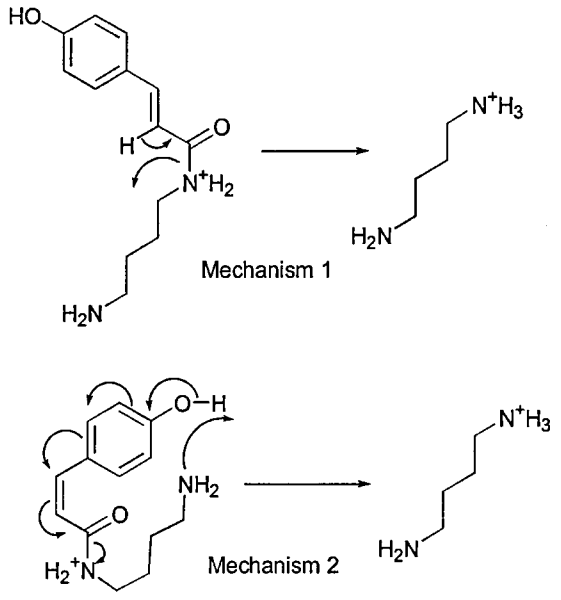

Figure 3.7

Both mechanisms involve an even number of bond cleavages (two for mechanism 1 and six for mechanism 2) so the originally charged atom is retained in the fragment ion in both cases. Mechanism 1 is a charge retention case whereas mechanism 2 involves charge migration to the other amino group. It must be noted that for mechanism 2 to occur a trans-cis isomerisation of the alkyl double bond must occur. This is another example of how bond rearrangements may occur prior to dissociation, often serving to complicate the interpretation of low energy CID spectra. The ESI MS/MS experiments were performed in CD_3OD and the labile H atoms were exchanged for D atoms. The fragment ion generated, with a mass of 89Da, would shift in mass to 93Da if it was produced as a result of mechanism 1 but would shift in mass to 94Da if produced as a result of mechanism 2. Both peaks were observed indicating that it is possible for both mechanisms to occur, although the peak at 94Da was more abundant than the peak at 93Da.[71]

Care must be taken when interpreting the results of such deuterium exchange experiments. It is probable that a quantity of H/D isotope scrambling may occur during the fragmentation process. Such scrambling has been observed in the CI/MS/MS and ESI/MS/MS spectra of tetrasubstituted polyketide δ-lactones.[72] The effect has also been observed in the CI spectra of cyclohexanol[73] and cycloheptanol.[74] The extent of hydrogen rearrangement prior to the fragmentation of CI generated deuterium labelled cyclohexyl derivatives increases with increasing proton affinity of the reagent gas. This means that a lowering of the internal energy of the ion results in increased bond rearrangements and atom scrambling prior to dissociation.[62]

The increase in H/D scrambling indicates that many rearrangements and hydride transfer steps may occur prior to bond cleavage. Without isotope labelling these rearrangements will remain undetected by mass spectrometry. Under low energy CID conditions the energy required for dissociation is built up gradually over multiple impacts with the collision gas. This provides ample time for rearrangement reactions, that only require a low activation energy, to take place. This is especially true in ion trap instruments where reaction times may be of the order of 3.5 ms, where the collision gas is usually helium and where the accelerating "tickle" voltage is no more than 5V.

Another aid in interpreting MS/MS spectra is the use of the accurate mass of an ion.[75] When the mass of an ion is known to within 5ppm it allows the determination of possible empirical formulae. The empirical formula of a fragment ion can assist in the elucidation of its structure. This is a technique that has not been extensively applied because of the difficulties in accurately calibrating an MS/MS spectrum. There are two methods that have been used in order to generate accurate mass calibrations of MS/MS spectra. The first is an iterative procedure that has been carried out on a FT-ICR mass spectrometer. An external calibration cannot be applied to a FT-ICR MS/MS spectrum because the presence of collision gas alters the observed masses of ions. Instead an internal calibration file is built up from the masses of known product ions in a MS/MS spectrum and this is used to calibrate the instrument. The masses of unknown product ions are guessed, and their masses are added to the list of calibration masses. If the guess is correct then the overall fit of the calibration line will be good. If the guess is incorrect then the overall fit of the calibration line will become worse. Eventually all unknown masses are brought into the calibration. The process is time consuming and relies on knowledge of the molecular structure in order to make guesses at the fragment ion masses of the initial calibration.[76]

A second method of accurate calibration may be applied to MS/MS spectra obtained on quadrupole-TOF (Q-Tof) hybrid instruments. The mass of the precursor ion can be used as a single reference point in order to calibrate internally an MS/MS spectrum.[77] In TOF instruments variation in observed mass occurs because of diurnal temperature changes that cause contraction and expansion of the metal flight tube. These changes are proportionate over the entire mass range so that a single reference mass may be used to correct the entire spectrum. It is only necessary to know the mass of a single peak in the MS/MS spectrum and this may be either the parent ion or a known fragment. The method is quick and straightforward and requires no guesswork in estimating the formulae of unknown fragments. However some knowledge of the structure of the analyte molecule is still required. At present there is no commonly used method of generating an accurate calibration of the MS/MS spectrum of a completely unknown molecule.

However, recent developments in the use of dual-probe electrospray systems have been described that make possible accurate mass MS/MS experiments on unknown compounds.[78] A FT-ICR mass spectrometer has been used to generate CID fragment ions of a 15-mer oligonucleotide. The fragment ions were trapped in the usual way whilst a second electrospray probe was used to generate ions of polyethylene glycol (PEG). These were trapped together with the fragment ions and the spectrum generated could be internally calibrated using the known masses of the PEG oligomers. The data obtained were accurate to within 5ppm but the method suffers from one main drawback. The time taken to complete the method is of the order of a few seconds, 4 seconds to accumulate the oligonucleotide ions followed by 0.5 seconds to accumulate the PEG ions. The ion isolation and CID steps also take a certain amount of time so the method is not compatible with real time LC/MS/MS analysis in complex mixtures, where good definition of chromatographic peaks is important.

A dual electrospray probe method has also been applied to the acquisition of accurate mass MS/MS spectra using a Q-TOF mass spectrometer.[79] The two electrosprays are kept separate by means of a mechanical rotor that eliminates interference between them and that allows either to be selected at pre-set intervals. One spray contains the reference compound and the other the analyte. The reference spray is periodically sampled and the spectrum is stored in a discrete data file. The analyte spectrum is then corrected using the known peak in the reference spectrum. The data are accurate to within 5ppm and the advantages of this method include the fact that it is compatible with high performance chromatography and that the MS/MS spectra are free from potentially interfering calibrant peaks. The technique was applied to the identification, by HPLC/MS/MS, of ibuprofen metabolites in human urine.

Chapter 4

Materials and Methods

Methanol, acetonitrile and water, used to dissolve and dilute the analytes prior to analysis by mass spectrometry, were of HPLC grade (Fischer Scientific UK Ltd., Loughborough, UK). Deuterium oxide at 99.9% D and deuterated methanol (CD_3OD) at 100% D (Acros Chemicals, Loughborough, UK.) were used in the deuterium labelling experiments. $H_2{}^{18}O$ at 99.9% ^{18}O was used for the stable isotope labelling of the C-9 carbonyl group.

An LCQ ion trap mass spectrometer (Finnegan MAT, San Jose, CA, USA) was operated in the positive-ion electrospray mode. Nitrogen was used as the source desolvation gas and helium as the collision gas within the trap. Nitrogen gas flow rates, electrospray capillary voltage, heated capillary temperature and tube lens voltage were optimised to give maximum signal intensity for the protonated analyte. The precursor ion isolation window was set to 5 Da in order to maximise transmission of ions to the CID and MS2 stages of the experiment.

A Q-Tof hybrid quadrupole/time of flight mass spectrometer (Micromass UK Ltd., Manchester, UK) was operated in the positive-ion electrospray mode. Nitrogen was used as the source desolvation gas and also as the collision gas within the hexapole collision cell. . Nitrogen gas flow rates, electrospray capillary voltage, source cone voltage and collision cell gas pressure were optimised to give maximum signal intensity for the protonated analyte. The precursor ion isolation window was set to 1 Da. For accurate mass experiments the ToF mass analyser was calibrated using a series of reference ions obtained from an infusion of polyethylene glycol. For accurate mass MS/MS experiments the precursor ion was used as an internal reference mass.

Erythromycin A, oleandomycin, clarithromycin and roxithromycin were purchased from Sigma-Aldrich Corp., St. Louis, MO, USA. *Sec*-butylerythromycin B was obtained by isolation from the fermentation of a strain of *Saccharapolyspora erythrea.*

For experiments involving H_2O and methanol approximately 1 mg of analyte was weighed out using an analytical balance. This was dissolved in sufficient methanol to give a concentration of 1 mg/mL stock solution. A 10 µL aliquot of the stock was diluted with 990 µL of a mixture of methanol and water (1:1, v/v) to give a 10 µg/mL solution.

For experiments involving deuterium oxide and deuterated methanol approximately 1 mg of analyte was weighed out using an analytical balance. This was dissolved in sufficient deuterated methanol to give a concentration of 1 mg/mL stock solution. A 10 μL aliquot of the stock was diluted with 990 μL of a mixture of deuterated methanol and deuterium oxide (1:1, v/v) to give a 10 μg/mL solution.

In order to investigate the part played by the C-9 carbonyl group in the first elimination of water the carbonyl oxygen was labelled with ^{18}O. Erythromycin A and *sec*-butylerythromycin B (0.5 mg each) were each dissolved in 100 μL of $^{18}OH_2$ and stored in a refrigerator for four days. An aliquot was taken and dissolved in HPLC grade acetonitrile to a concentration of 10 ug/mL.

Chapter 5

CID reactions of the Erythromycins

Initial experiments were carried out on a solution of erythromycin A (Sigma E 6376) at 10ug/mL in methanol. The sample was infused into the standard ESI source of an LCQ ion trap mass spectrometer (Finnegan MAT, San Jose, CA, USA) at a rate of 10 uL/min and a series of sequential tandem mass spectrometry experiments were carried out up to MS^5. Whereas the initial MS/MS spectrum of the $[M+H]^+$ ion at 734 Da is very difficult to interpret (Figure 5.1), the resulting MS^n spectra can be used to generate a diagram of the genealogy of fragment ions from their higher mass precursors. A diagram showing the major fragment ions is shown (Figure 5.2). This can help in deconvoluting the fragmentation sequences that occur.

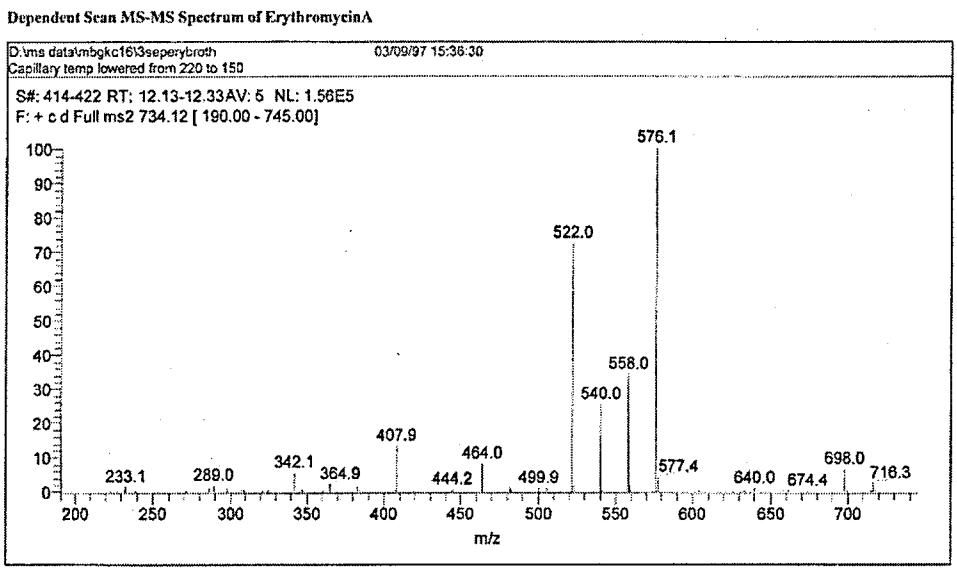

Figure 5.1

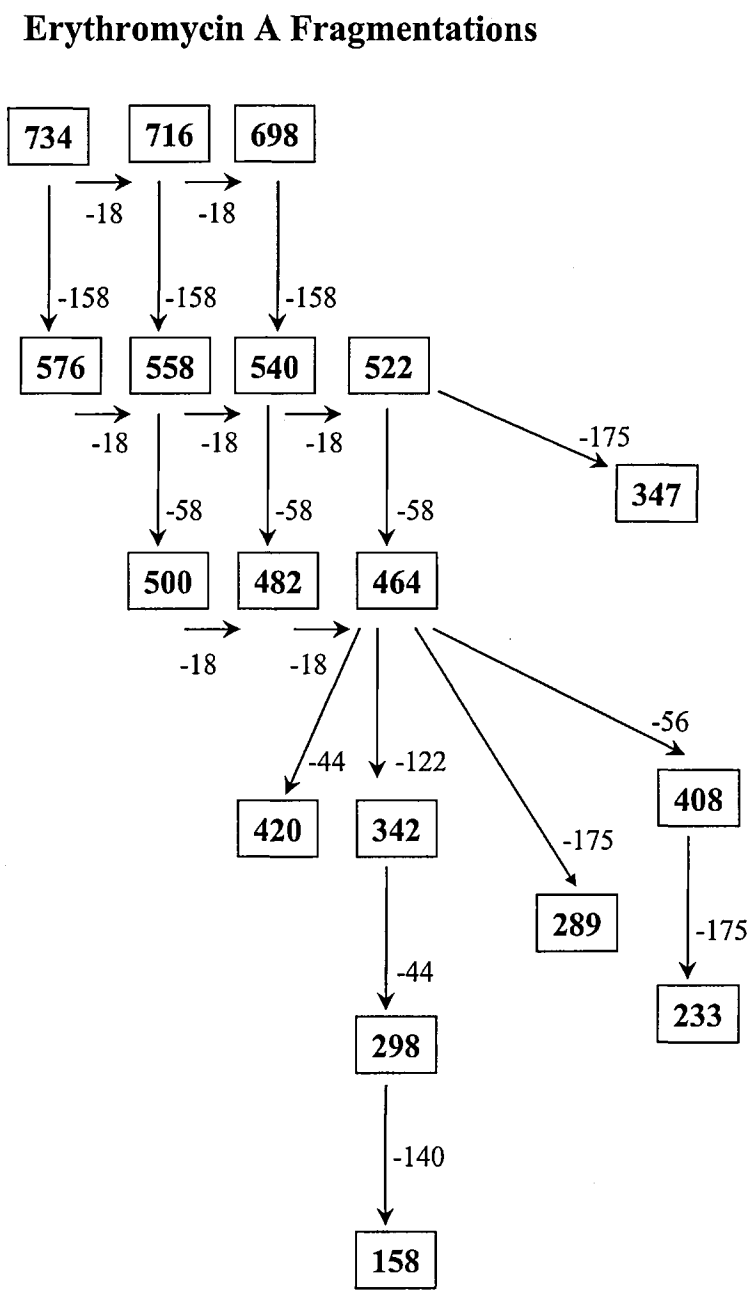

Figure 5.2

It can be seen that the ions that appear in the MS^n experiments are also seen in the initial MS/MS spectrum of the ion at 734 Da. All losses are expected to be neutral molecules. It is unlikely that radical ions would be generated in the low energy CID conditions employed. This means that any odd-mass losses must contain an odd number of nitrogen atoms and

this allows the location of the desosamine sugar to be tracked through the fragmentation scheme.

Two fragmentation reactions compete in the decomposition of the pseudomolecular ion at 734 Da, loss of the cladinose sugar (-158 Da) to yield a product ion at 576 Da and loss of H_2O (-18 Da) to yield a product ion at 716 Da. The loss of the cladinose sugar proceeds via a charge remote fragmentation mechanism and, prior to this study, was the only fragmentation reaction of erythromycin A that had been explained (Figure 3.3). Three losses of H_2O occur together with loss of the cladinose sugar. Once the sugar and the first water is lost the ions are able to lose an unknown fragment with a mass of 58 Da. Once the three waters, the sugar and the loss of 58 Da have occurred the fragment ion at 464 Da is generated. From here four reactions compete, with losses of 44 Da, 122 Da, 175 Da and 56 Da. The loss of 44 Da together with the loss of 122 Da generates an ion with a mass of 298 Da. This loses 140 Da to generate an ion corresponding to the desosamine sugar residue. The loss of 56 Da from the 464 Da ion produces a fragment ion with a mass of 408 Da.

Since all the fragment ions described so far are of even mass they must contain the amino sugar moiety and this is consistent with the assumption that the location of the charge proton is on the nitrogen atom of the desosamine sugar. This is in keeping with the NMR spectroscopy study of Gharbi-Benarous et al. who showed that the chemical shifts of the N,N-dimethyl protons depend on the pH of the D_2O solution in which the experiments were conducted.[80] At high pH rotation occurs about the C3'-N bond, the two methyls are equivalent and only a single signal is observed. At low pH hydrogen bonding, probably between the 2'-OH and the 3'-$NH^+(Me)_2$, hinders the free rotation of the C3'-N bond (Figure 5.3). At low pH two distinct methyl signals are observed.

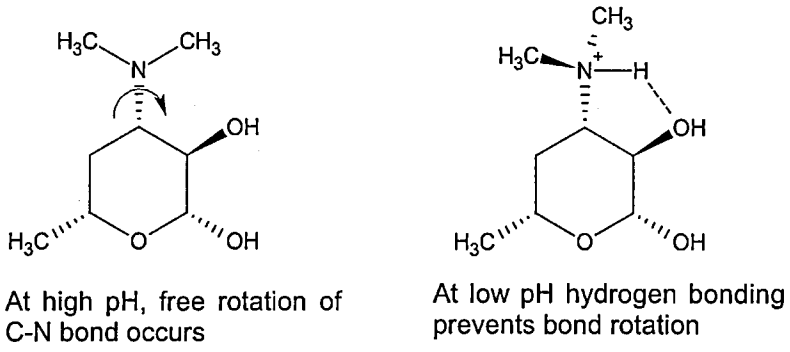

At high pH, free rotation of C-N bond occurs

At low pH hydrogen bonding prevents bond rotation

Figure 5.3

However, if during CID fragmentation of the molecule the charge were to remain on the nitrogen atom then it would mean that most of the fragmentation reactions of erythromycin A are of the charge remote type. This seems unlikely and some reaction routes indicate that the charge proton does not remain on the amino nitrogen. The ions at 558 Da, 540 Da and 522 Da each lose 175 Da to give fragments with masses 383 Da, 365 Da and 347 Da respectively. The 408 Da and the 464 Da ions also lose 175 Da to yield ions at 289 Da and 233 Da. The mass of 175 Da corresponds to the neutral loss of the desosamine sugar group. The fact that the desosamine sugar can be lost as a neutral fragment may be explained in terms of some form of pre-dissociative rearrangement reaction that transfers the charge to the macrolide ring.

In order to understand the later ring opening reactions that occur, it seems necessary to first understand the nature of the three initial losses of water. A reasonable assumption would be that the three losses of water occur from the three hydroxyl groups on the macrolide ring, via a concerted mechanism (Figure 5.4). However, the matter is complicated by the fact that the loss of the cladinose sugar generates a fourth hydroxyl group at the C-3 position of the 576 Da ion (Figure 5.5). If a charge remote elimination were the mechanism of the three losses of water then an important question is, which of the four hydroxyl groups remains?

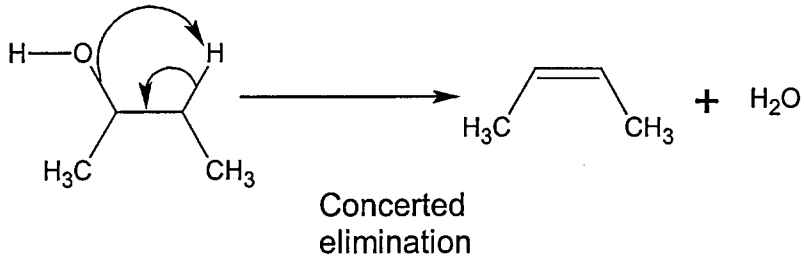

Figure 5.4

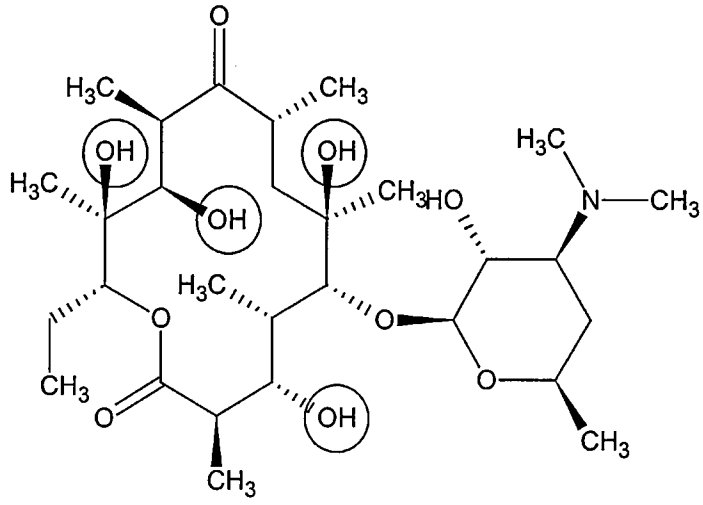

Figure 5.5

Experiments in Deuterated Solvents and Accurate Mass MS/MS Data of Erythromycin A

In order to investigate whether the fourth hydroxyl group is involved in one of the three losses of water the above experiments were repeated in a 1:1 mixture of D_2O/CD_3OD. The exchangeable protons were exchanged for deuterons and sequential tandem mass spectrometry experiments conducted on the mass shifted $[M+D]^+$ ion was used in an attempt to determine the number of exchangeable protons in the fragment ions.

However, when using the LCQ mass spectrometer to isolate precursor ions to a 1Da window very weak spectra were obtained, although a large number of scans could be combined to give consistent spectra.

In order to check the results obtained on the low-resolution LCQ the experiments were repeated on a Q-Tof hybrid quadrupole-ToF mass spectrometer (Micromass, Manchester, UK.). The Q-Tof is capable of isolating a monoisotopic precursor ion so the deuterium labelled MS^n experiments were repeated on this instrument. The relative abundances of the various fragment ions are different to those obtained from the LCQ ion trap, indicating that the deposition of collisional energy into the parent ion is not the same for these two instruments. The mass shifted fragmentation scheme is shown (Figure 5.6).

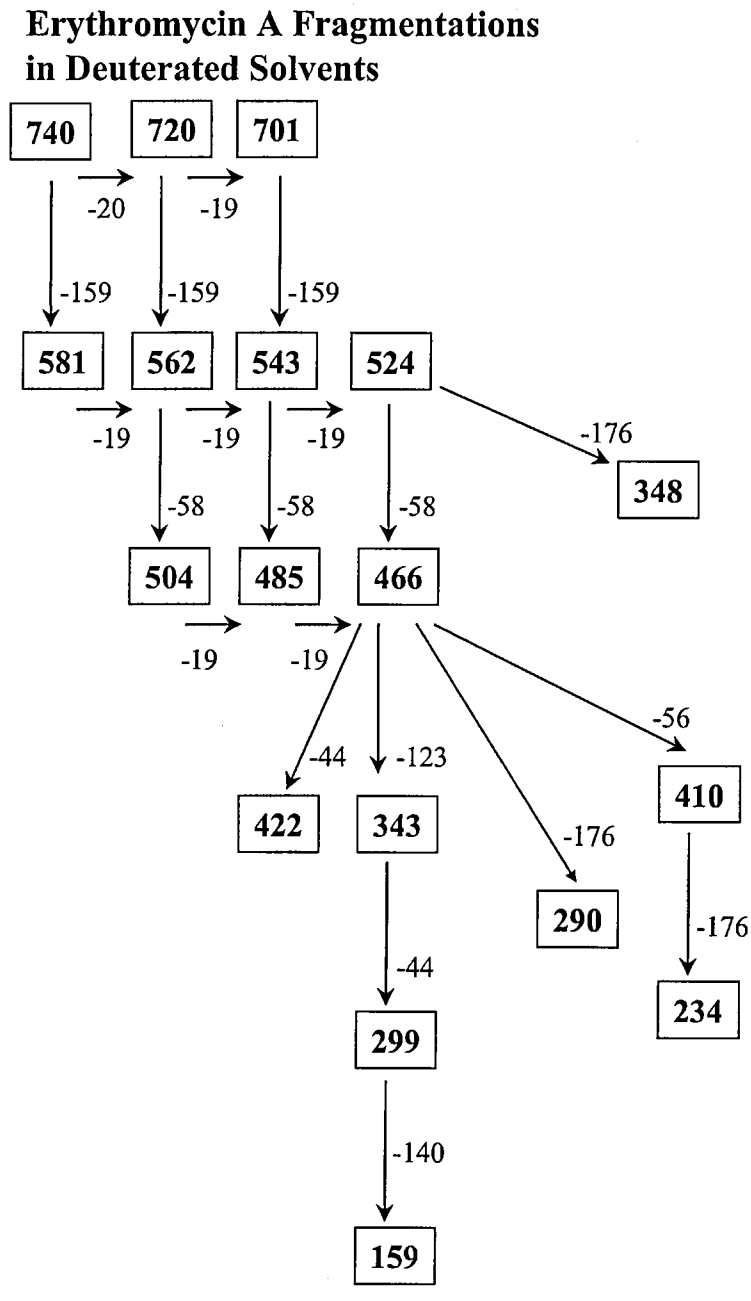

Figure 5.6

Accurate mass information was also obtained on the Q-Tof. The peak at 734 Da in the non-deuterated sample was monoisotopically isolated and fragmented using argon as a collision gas, at a collision energy of 20 V. The spectrum obtained shows the whole of the mass range of interest (Figure 5.7).

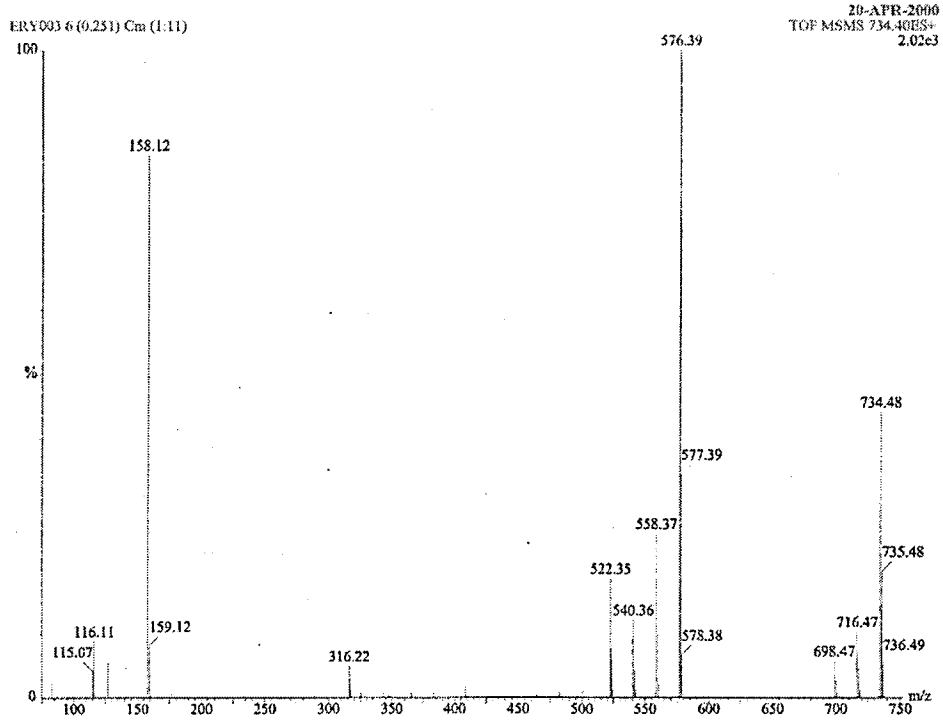

Figure 5.7

There is no low-mass cut-off at 1/3 the parent mass, as seen on the LCQ. Also, there is a fragment ion at 316 Da that is not observed in the ion-trap MS/MS spectra. This is possibly from a fragmentation mechanism that requires a higher activation energy than that possible in the ion trap.

The Q-Tof MS/MS spectrum was internally corrected using the exact mass of the parent ion as a single reference point (lock mass). The accurate mass information obtained enables the elemental composition of fragment ions and neutral losses to be determined and these are shown (Table 5.1). The peaks at 298 Da and 289 Da do not appear with sufficient abundance for accurate mass determination in the Q-Tof mass spectrum. The accurate mass values for these ions were determined using a BioApex FT-ICR mass spectrometer (Bruker Daltonics, Billerica, MA. USA) and are taken from the PhD thesis of Dr. Paul Gates.[81]

Table of Erythromycin Fragment-Ion Accurate Masses

Observed Mass	Theoretical Mass	ΔMass in mDa	ΔMass in ppm	Elemental Composition
716.4590	716.4585	0.5	0.7	$C_{37}H_{66}NO_{12}$
698.4490	698.4479	1.1	1.6	$C_{37}H_{64}NO_{11}$
576.3751	576.3748	0.3	0.5	$C_{29}H_{54}NO_{10}$
558.3658	558.3642	1.6	2.8	$C_{29}H_{52}NO_{9}$
540.3547	540.3536	1.1	2.0	$C_{29}H_{50}NO_{8}$
522.3440	522.3431	-0.9	-1.7	$C_{29}H_{48}NO_{7}$
500.3241	500.3223	1.8	3.5	$C_{26}H_{46}NO_{8}$
482.3103	482.3118	-1.5	-3.1	$C_{26}H_{44}NO_{7}$
464.3023	464.3012	1.1	2.3	$C_{26}H_{42}NO_{6}$
408.2763	408.2750	1.3	3.2	$C_{23}H_{38}NO_{5}$
383.2445	383.2434	1.1	3.0	$C_{21}H_{35}O_{6}$
365.2343	365.2328	1.5	4.1	$C_{21}H_{33}O_{5}$
347.2243	347.2222	2.1	5.9	$C_{21}H_{31}O_{4}$
342.2290	342.2280	1.0	2.8	$C_{18}H_{32}NO_{5}$
316.2135	316.2124	1.1	3.6	$C_{16}H_{30}NO_{5}$
233.1556	233.1542	1.4	6.0	$C_{15}H_{21}O_{2}$
176.1278	176.1287	-0.9	-5.1	$C_{8}H_{18}NO_{3}$
158.1187	158.1181	0.6	3.8	$C_{8}H_{16}NO_{2}$
116.1076	116.1075	0.1	0.4	$C_{6}H_{14}NO$

	RMS Average	1.1	3.4	
289.1810	289.1798	1.2	4.0	$C_{18}H_{25}O_3$
298.2374	298.2377	-0.3	-0.8	$C_{17}H_{32}NO_3$

Table 5.1

Inferences from Accurate Mass and Deuterium Labelling of Erythromycin A

The information gained from the deuterium labelling experiment is invaluable when attempting to decipher the fragmentations that occur. Consistent with previous reports there is some degree of isotopic scrambling that occurs under CID conditions, but the most abundant peaks in the cluster are taken as representative of the amount of deuterium labelling present in the fragment ion. Given the labelling and accurate mass data the following conclusions can be drawn. For clarity a numbered structure of erythromycin A is shown (Figure 5.8).

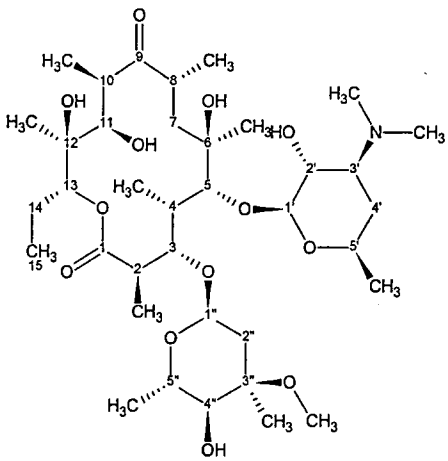

Figure 5.8

- The first loss of water from the pseudomolecular ion is shifted to loss of D_2O. This might indicate either an E1 type mechanism of elimination or the occurrence of some form of rearrangement prior to elimination. The second loss of water is shifted to loss of HDO consistent with a charge remote, concerted elimination mechanism.

- The three losses of water that occur after the loss of cladinose are all shifted to loss of HDO. A certain amount of pre-dissociative isotope scrambling may occur in order to produce this result.

- The loss of the cladinose sugar as a neutral molecule is consistent with the expected charge remote mechanism.

- The loss of 58 Da corresponds to loss of C_3H_6O and it does not contain an exchangeable proton. The only likely region of the molecule corresponding to this seems to be the C-13 to C-15 starter-unit.

- The loss of 44 Da corresponds to loss of CO_2 from the C-1 ester bond region of the molecule. It is interesting that this seems to occur after the lactone ring oxygen is lost, and so the CO_2 unit must be regenerated with an oxygen atom from elsewhere on the macrolide ring.

- The loss of 122 Da corresponds to loss of $C_8H_{10}O$, a molecule with a double bond equivalent of 4, the same as that of a benzene ring. The fragment shifts to loss of 123 Da in deuterated solvents indicating that it contains an exchangeable proton. This proton may be on the hydroxyl group that is not lost as a water elimination in the earlier fragmentations. A likely part of the molecule that corresponds to the 122 Da loss is the C-8 to C-12 region.

- The loss of 56 Da from the ion at 464 Da does not shift in mass in deuterated media and it has the elemental composition C_3H_4O. It probably corresponds to loss of the C-1 to C-2 portion of the molecule.

- The loss of 140 Da from the ion at 298 Da does not change in mass in deuterated media. It probably corresponds to the remaining C-3 to C-7 portion of the macrolide ring.

- The losses of 175 Da that equate to loss of the desosamine sugar shift in mass by 1 Da in deuterated media, consistent with the one exchangeable hydroxyl group in the sugar.

MS/MS data for sec-Butylerythromycin B in both Normal and Deuterated Solvents

LCQ MS^n studies in normal solvents were next carried out on *sec*-butylerythromycin B, an analogue of erythromycin B that contains a *sec*-butyl starter acid unit (Figure 5.9).

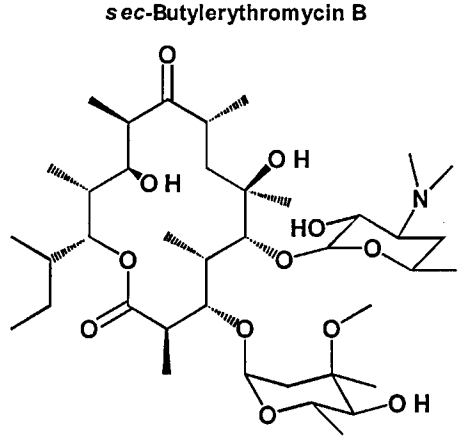

Figure 5.9

The fragmentation reactions of the pseudomolecular ion at 746 Da are similar to those of the erythromycin A ion of 734 Da (Figure 5.10).

Sec-Butylerythromycin B Fragmentations

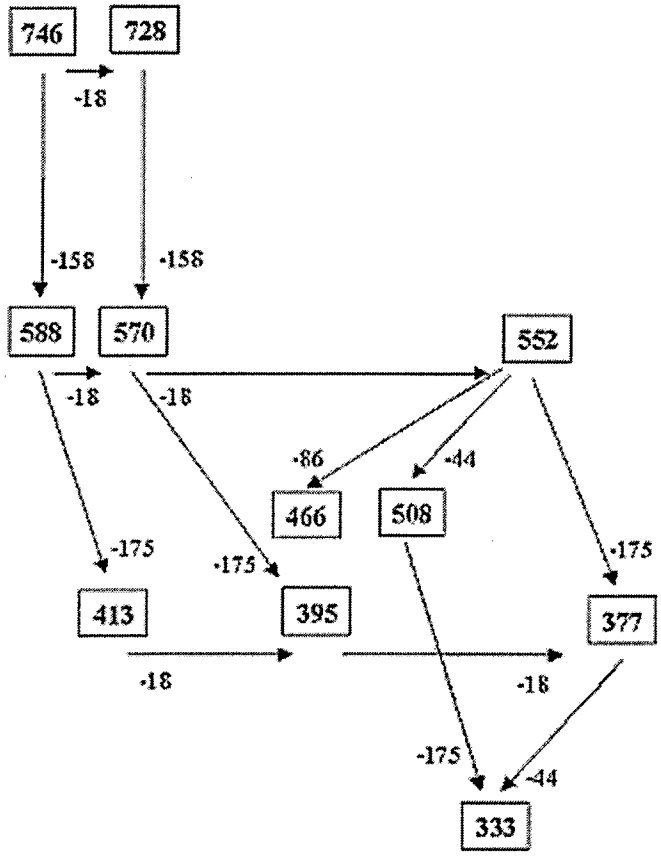

Figure 5.10

It loses the cladinose sugar easily and, since there is one less hydroxyl group on the macrolide ring, it only easily loses two water molecules. This confirms that the C-12 hydroxyl group is lost as a water elimination from the 734 Da ion of erythromycin A.

From the ion at 552 Da a loss of 44 Da occurs that corresponds to the loss of CO_2, in competition with a loss of 86 Da which corresponds to the *sec*-butyl starter unit. The loss of 86 Da is a minor fragmentation pathway but it reinforces the conclusion that the loss of 58 Da in the fragmentation scheme of erythromycin A is due to an analogous loss of the propionate starter acid unit. The major fragmentation routes after loss of cladinose and the two waters seems to be loss of the desosamine sugar, a route that also occurs in the CID of erythromycin A.

An MS/MS experiment was also conducted on *sec*-butylerythromycin B in deuterated solvents. The most significant information from this experiment is that the loss of the first water shifts from loss of H_2O (-18 Da) to loss of D_2O (-20 Da). This suggests that the same

mechanism of water elimination occurs in both *sec*-butylerythromycin B and erythromycin A and that it is not related to the C-12 hydroxyl group.

MS/MS of Related Molecules

An MS/MS experiment was conducted on oleandomycin (Sigma O 6125), a member of the erythromycin family produced by the bacterium *Streptomyces antibioticus.* It lacks the hydroxyl groups at the C-6 and C-12 positions, has an epoxy substituent at the C-8 position, an acetate starter unit and an oleandrose sugar in place of cladinose at the C-3 position. An MS/MS experiment was also conducted on roxithromycin (Sigma R 4393), a synthetic modification of erythromycin A that contains an oxime group in place of the C-9 carbonyl (Figure 5.11).

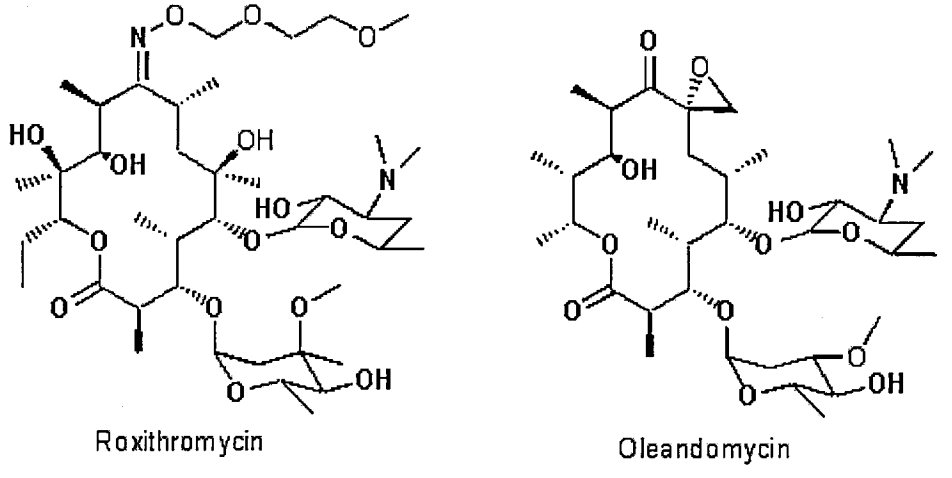

Figure 5.11

The fragmentation schemes of these two molecules are shown (Figure 5.12).

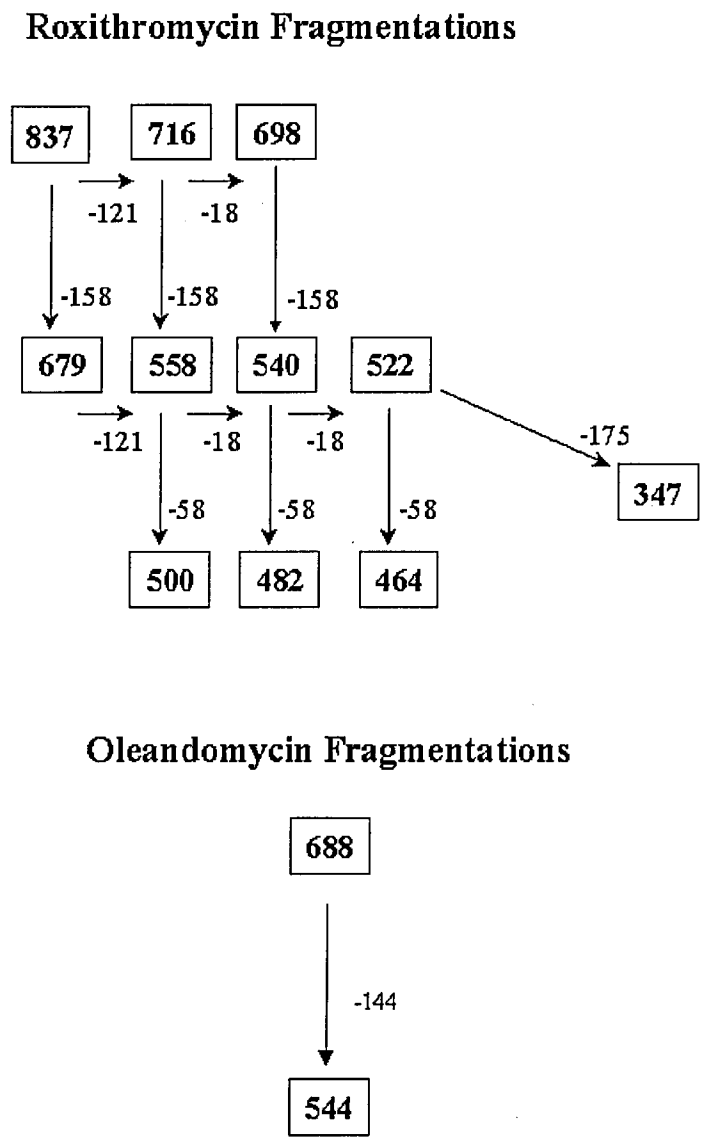

Figure 5.12

The MS/MS analysis of oleandomycin shows no water loss from the pseudomolecular $[M+H]^+$ ion at 688 Da. The only fragment observed is the loss of 144 Da, which corresponds to the oleandrose sugar. The C-11 hydroxyl group is not eliminated as water and this may also be the hydroxyl that is not eliminated as water in the fragmentation of erythromycin A.

The MS/MS analysis of roxithromycin shows no loss of water from the pseudomolecular $[M+H]^+$ ion at 837 Da. Instead the loss of cladinose competes with loss of the C-9 oxime group. The rest of the fragmentation of roxithromycin is exactly the same as for erythromycin, indicating that loss of the oxime group leaves a product ion at 716 Da which has the same structure as the 716 Da ion in the MS/MS spectrum of erythromycin A. The inference is that the first loss of water from the erythromycin A pseudomolecular ion is analogous to loss of the oxime from roxithromycin and is from the C-9 carbonyl group.

The loss of D_2O that occurs in both erythromycin A and *sec*-butylerythromycin B are unlikely to be as a result of elimination of either the C-11 or the C-12 hydroxyl groups, it is very probably associated with the C-6 hydroxyl group.

^{18}O Labelling Experiments and MS/MS of Clarithromycin

In order to investigate the part played by the C-9 carbonyl group in the first elimination of water the carbonyl oxygen was labelled with ^{18}O. Erythromycin A and *sec*-butylerythromycin B (0.5 mg each) were each dissolved in 100 uL of $^{18}OH_2$ and stored in a refrigerator for four days. An aliquot was taken and dissolved in HPLC grade acetonitrile to a concentration of 10 ug/mL. These samples together with untreated controls were analysed on a Q-Tof mass spectrometer.

Dissolving the samples in $^{18}OH_2$ allows the exchange of ^{18}O into the C-9 carbonyl by a mechanism involving the reversible formation of a gem diol (Figure 5.13).

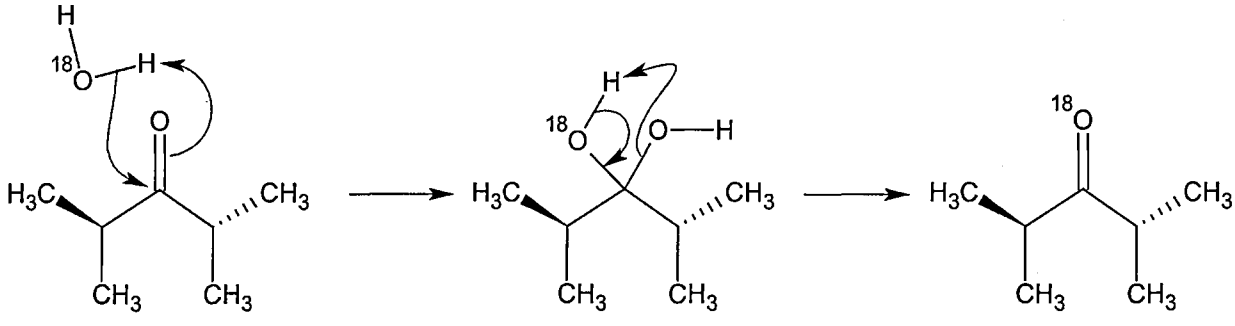

Figure 5.13

When the $[M+H]^+$ +2 Da peak from an untreated sample (736 Da peak for erythromycin A, 748 Da peak for *sec*-butylerythromycin B) was analysed by MS/MS the first loss of water is – 18 Da which corresponds to loss of $^{16}OH_2$ (Figure 5.14, 5.15).

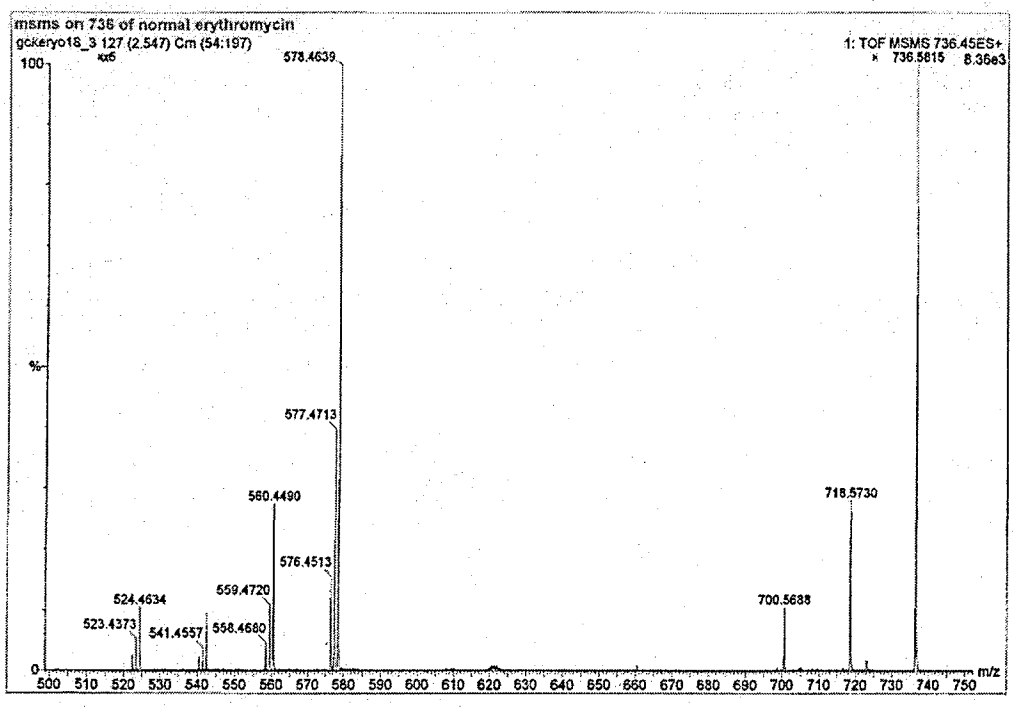

Figure 5.14

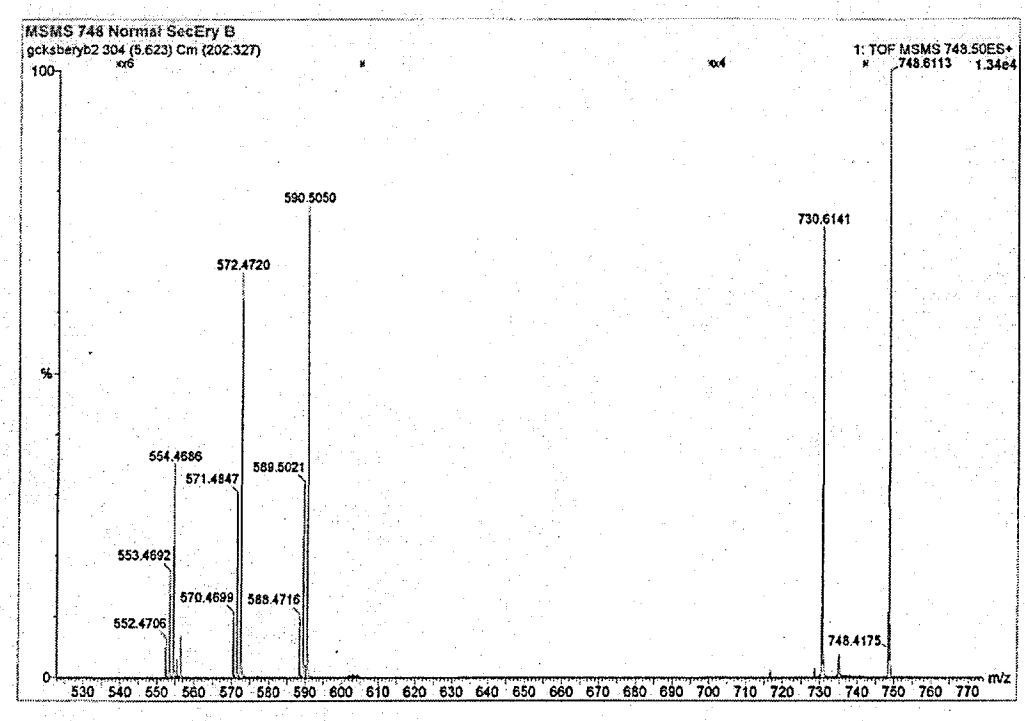

Figure 5.15

This is because the $[M+H]^+$+2 Da peak mostly consists of ^{13}C and D isotopes with very little ^{18}O. When the same experiments are performed on the enriched samples it can be seen that the $[M+H]^+$+2 Da peaks are enhanced in ratio. The fragment ions corresponding to loss of 18 Da are still in evidence, since the isolated precursor is a mixture of enriched and naturally occurring isotopes, but the MS/MS spectrum now shows a clear peak for loss of 20 Da (716 Da for erythromycin A, 728 Da for *sec*-butylerythromycin B) (Figure 5.16, 5.17).

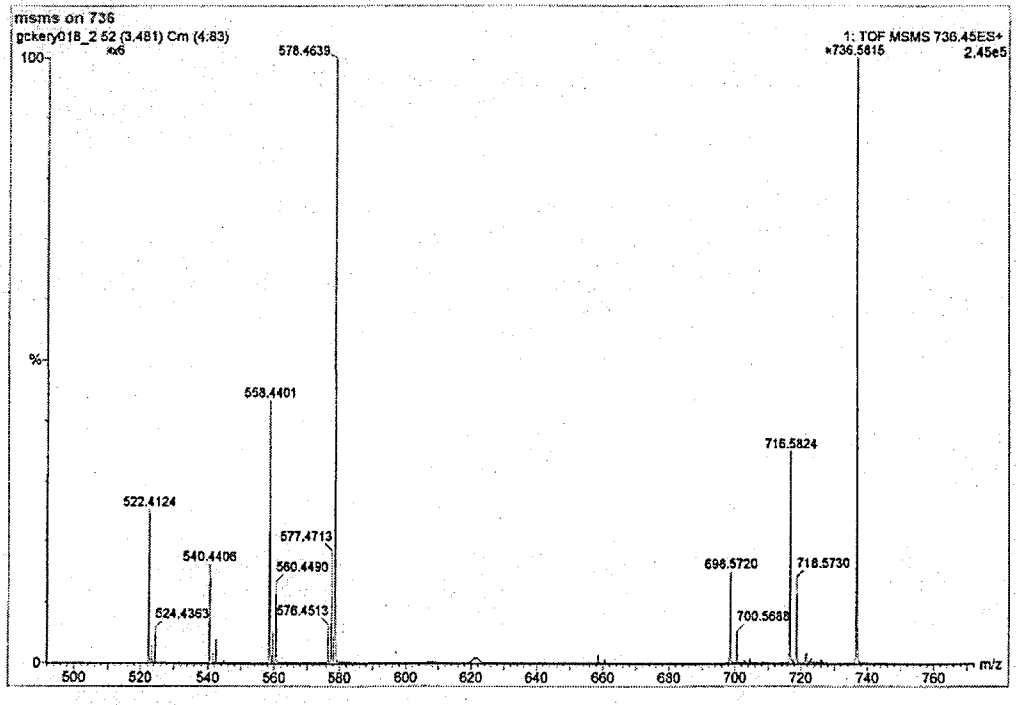

Figure 5.16

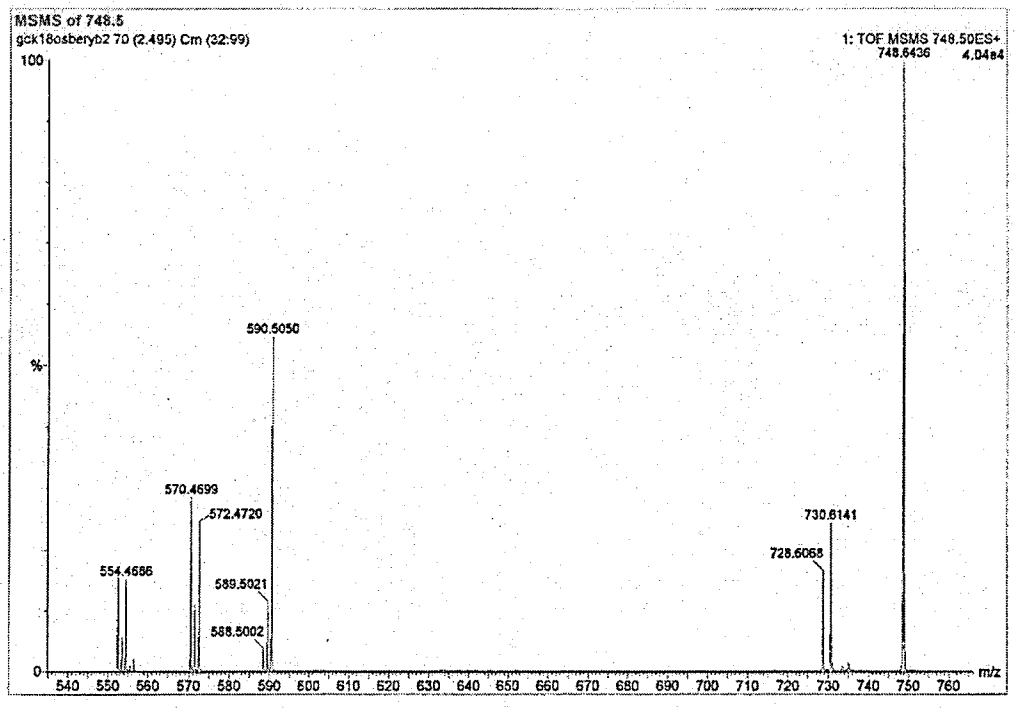

Figure 5.17

This indicates that the first water loss has shifted in mass and can only be from the C-9 position carbonyl group. Given that two exchangeable protons are involved in this neutral loss and that it also occurs in *sec*-butylerythromycin B, which lacks a hydroxyl group at the C-12 position, a mechanism is given which results in the formation of an oxonium ion (Figure 5.18). This involves attack by the C-6 hydroxyl group onto the C-9 carbonyl group (possibly protonated) to give a hemiacetal that, after proton transfer, can lose water.

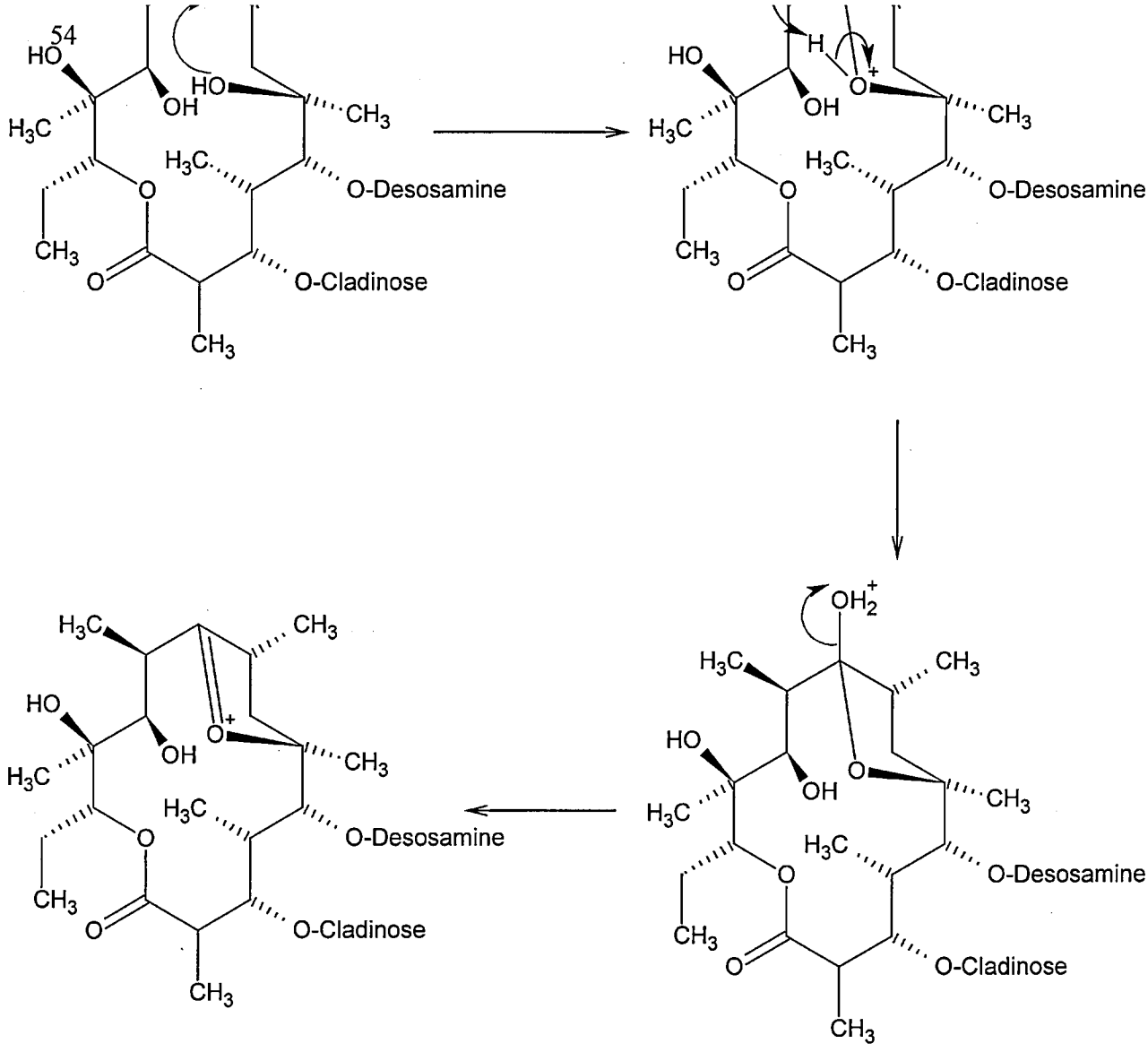

Figure 5.18

This oxonium ion is similar in structure to that of erythromycin A enol ether, as determined by NMR spectroscopy (Figure 5.19).[82] Erythromycin A enol ether is formed as a decomposition product of erythromycin A under acid hydrolysis.

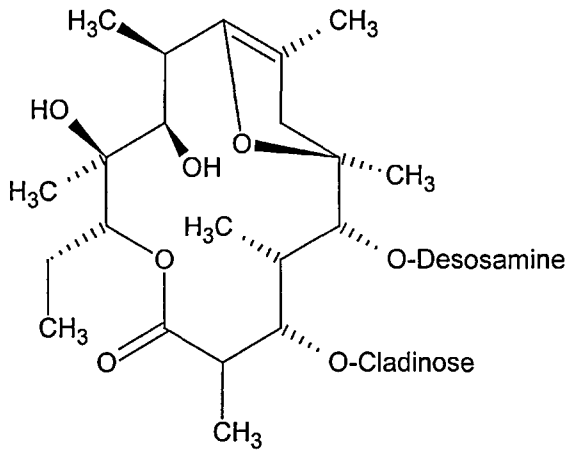

Erythromycin A enol ether

Figure 5.19

In order to further investigate the role of the C-6 hydroxyl in the fragmentation of the erythromycins a final experiment was performed on clarithromycin, the C-6 methyl ether of erythromycin A. Some of the neutral losses are similar to those of erythromycin A; for example there is a loss of 58 Da that may correspond to the polyketide starter unit. There are only two facile loses of H_2O, the desosamine sugar is more easily lost as a neutral fragment and there is a strong tendency to eliminate MeOH, presumably from the C-6 position. The ring opening reactions of erythromycin A do not occur. The fragmentation scheme for this molecule is shown (Figure 5.20).

Clarithromycin A Fragmentations

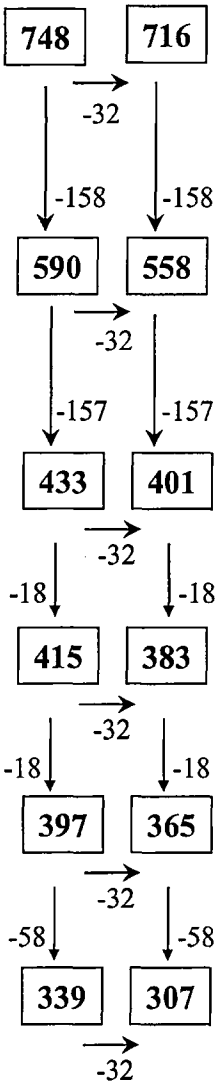

Figure 5.20

The results for clarithromycin indicate that the C-6 OH group is important in initiating many of the fragmentation reactions of erythromycin A.

The exact sequence of events in the dissociation of erythromycin A cannot be definitely known because of the extent of rearrangement reactions that undoubtedly occur during the process. However the following is postulated as plausible given the data available (Figure 5.21), starting from the oxonium ion shown in Figure 5.20, after one H_2O loss.

The loss of the cladinose sugar group competes with the first two losses of H_2O. One of these losses of water is from the C-9 keto group. The other is possibly from the C-12 hydroxyl group. In the postulated mechanism the C-12 hydroxyl group migrates to C-9 before elimination as water, resulting in migration of the charge to C-12. A third loss of H_2O only occurs after elimination of the cladinose sugar, evidence that it arises from the hydroxyl group at C-3 that is generated by the sugar loss.

After the cladinose sugar and three molecules of water are lost the fragment ion at 522 Da is generated. It is proposed that the C-13 to C-15 portion of the ion is lost next, via the mechanism shown, leaving an oxonium ion at 464 Da. The reaction sequence possibly branches at this point. The ion undergoes a neutral loss of 56 Da, probably corresponding to the C-1 to C-2 portion of the macrolide ring, in order to give the ion at 408 Da.

The ion at 464 Da also loses 122 Da, to give an ion at 342 Da. An elaborate series of rearrangements must take place for this to occur and the nature of these can only be guessed. The reactions shown leading up to the loss of 122 Da are purely speculative.

Another neutral loss that is difficult to decipher is the elimination of CO_2 from the ion at 342 Da. The scheme shows the hydroxyl group at C-6 migrating to C-1 in order for this loss to occur. Whilst this migration most probably occurs the mechanism by which it occurs is unknown and the reactions shown are speculative.

Finally the remaining portion of the macrolide ring is lost leaving the charge on the amino sugar at 158 Da.

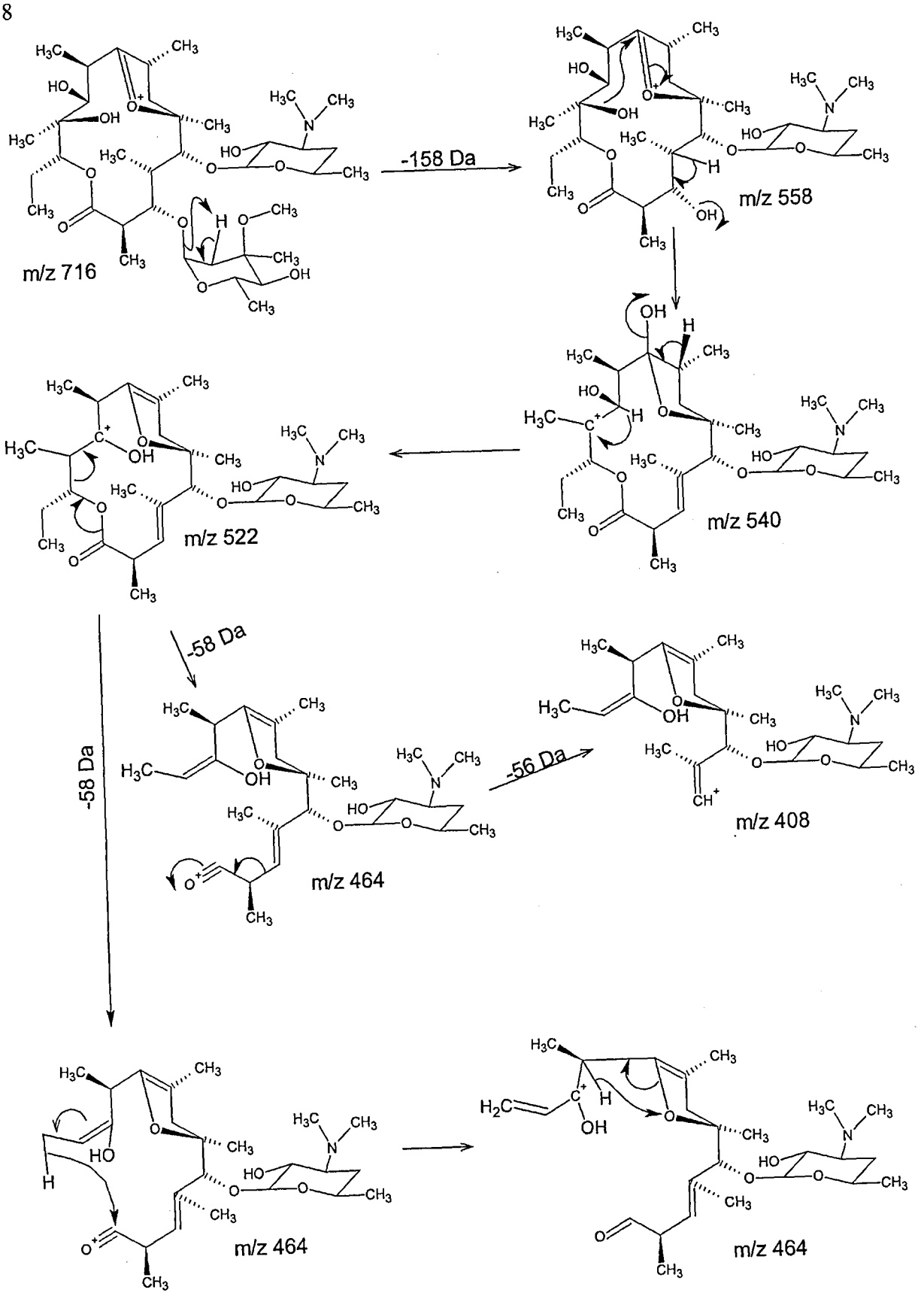
m/z 716
-158 Da
m/z 558
m/z 540
m/z 522
-58 Da
-58 Da
-56 Da
m/z 464
m/z 408
m/z 464
m/z 464

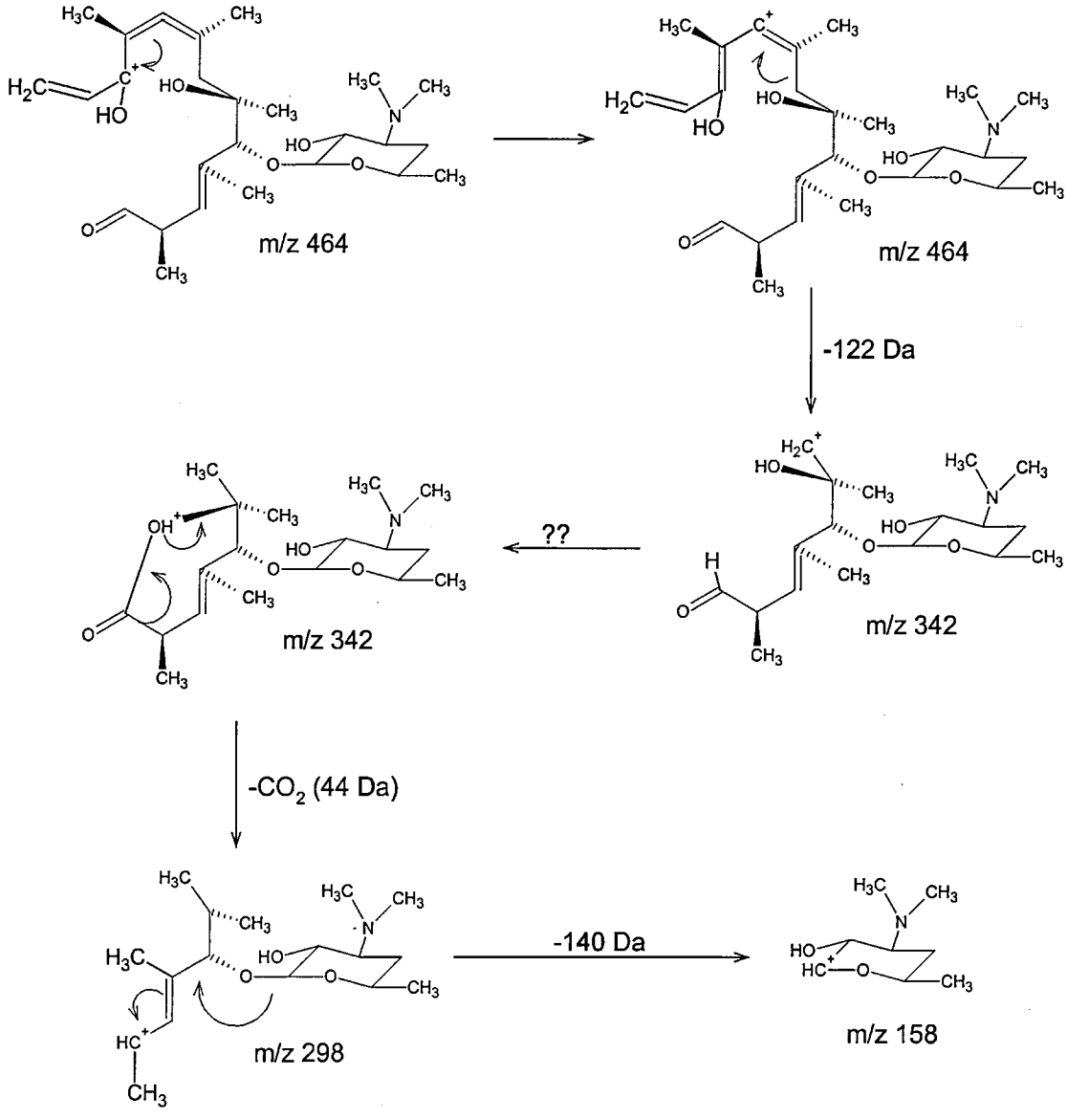

Figure 5.21

Chapter 6

Conclusions and Suggestions for Further Study

The first subject for future study should be the nature of the peak at 316 Da in the MS/MS spectrum obtained on the Q-Tof but not on the LCQ mass spectrometer. Preliminary experiments were performed in an attempt to characterise this fragment. CID fragment ions were generated by the use of a high sampling-cone voltage in the source of the Q-Tof. The peaks at 716 Da, 522 Da and 316 Da were selected for MS/MS analysis. The 716 Da precursor ion produced a fragment at 316 Da but the 522 Da precursor did not. The 316 Da precursor ion produced a fragment at 158 Da matching, to within 5 ppm, the accurate mass of the desosamine fragment ion.

Given that CID of both erythromycin A and clarithromycin produce the peak at 316 Da it cannot contain any part of the molecule from C-6 onwards. Since it is produced before its loss, it may contain a portion of the cladinose sugar. There is also the intriguing possibility that the 316 Da ion consists of the two sugar moieties as a disaccharide, having undergone rearrangement and loss of the entire macrolide ring. The accurate mass of the fragment matches to the correct elemental composition for this but the possible mechanism of such a rearrangement is not postulated.

Further experiments that need to be carried out include an investigation of the MS/MS product ions of erythromycin obtained under negative ion electrospray conditions. Although the basic amino group on the molecule ensures the formation of abundant positive ions negative ion spectra may also be obtained and these may yield useful structural information.

Also MS/MS experiments need to be carried out on positive ions obtained by sodium rather than proton adduction to the molecule. Sodiated ions are usually more stable than protonated ones and require higher activation energies before dissociation takes place, but the extent of pre-dissociative rearrangements that occur can be less. The work of Brull and co-workers demonstrated that MS/MS of a protonated oligosaccharide ion generates fragment ions formed by rearrangement and loss of an internal residue. Such ions complicate the MS/MS spectrum and lead to uncertainty in the assignment of the oligosaccharide sequence. When CID was performed on a sodiated oligosaccharide ion internal residue loss did not occur and the spectrum was much simpler to interpret.[83] A reason for this may be that the sodium cation is less able to take part in charge driven rearrangement reactions. This would have the effect of limiting low energy fragmentation

routes that require pre-dissociative rearrangements, making the ion more stable and more prone to charge remote fragmentation mechanisms. Sodiated MS/MS spectra may yield further useful structural information.

In conclusion, the techniques of sequential tandem mass spectrometry, isotope labelling and accurate mass tandem mass spectrometry can be employed to study the intramolecular fragmentation reactions that occur during the collision induced dissociation of complex, polyfunctional organic ions. An understanding of such reactions can aid in the interpretation of mass spectra from novel but structurally related compounds. The mass spectrometric techniques described above are compatible with high-throughput HPLC screening experiments.

References

1)Mann J. *Secondary Metabolism*; Second ed.; Clarendon Press: Oxford, 1987.

2)Staunton J.; Wilkinson B. *Chem. Rev.* **1997**, *97*, 2611-2629.

3)Staunton J.; Wilkinson B. *Top. Curr. Chem.* **1998**, *195*, 49-92.

4)Celmer W.D. *J. Am. Chem. Soc.* **1965**, *87*, 1801.

5)McGuire J.M.; Bunch R.L.; Anderson R.C.; Boaz H.E.; Flynn E.H.; Powell M.; Smith J.W. *Antibiot. and Chemotherapy* **1952**, *2*, 281.

6)Cocoran J.W.; Vygantas A.M. *Biochem.* **1982**, *21*, 263.

7)Donadio S.; Staver M.J.; McAlpine J.B.; Swanson S.J.; Katz L. *Science* **1991**, *252*, 675.

8)Cortes J.; Wiesmann K.E.H.; Roberts G.A.; Brown M.J.B.; Staunton J.; Leadlay P.F. *Science* **1995**, *268*, 1487.

9)Oliynyk M.; Brown M.J.B.; Cortes J.; Staunton J.; Leadlay P.F. *Chem. Biol.* **1996**, *3*, 833.

10)Leadlay P.F.; Staunton J.; Marsden A.F.A.; Wilkinson B.; Dunster N.J.; Cortes J.; Oliynyk M.; Hanefeld U.; Brown M.J.B. *Industrial Micro-Organisms, Basic and Applied Molecular Genetics*; American Society for Microbiology: Washington DC, 1997.

11)Pacey M.S.; Dirlam J.P.; Geldart R.W.; Leadlay P.F.; McArthur H.A.I.; McCormick E.L.; Monday R.A.; O'Connell T.N.; Staunton J.; Winchester T.J. *J. Antibiot.* **1998**, *51*, 1029-1034.

12)Jacobsen J.R.; Hutchinson C.R.; Cane D.E.; Khosla C. *Science* **1997**, *277*, 367-369.

13)Staunton J. *Curr. Opin. Chem. Biol.* **1998**, *2*, 339-345.

14)Cane D.E.; Walsh C.T.; Khosla C. *Science* **1998**, *282*, 63.

15)McDaniel R.; Thamchaipenet A.; Gustafsson C.; Hong Fu; Betlach M.; Betlach M.; Ashley G. *Proc. Natl. Acad. Sci. USA* **1999**, *96*, 1846-1851.

16)Khosla C. *Chemtracts-Org. Chem.* **1998**, *11*, 1-15.

17)Leadlay P.F *Curr. Opin. Chem. Biol.* **1997**, *1*, 162-168.

18) Shiou-Chuan T., Miercke L. J. W., Krucinski J., Gokhale R., Chen J., Foster P. G., Cane D. E., Khosla C., and Robert M. PNAS, **2001**, *98*, *26*, 14808-14813.

19) Pfeifer B, Hu Z, Licari P, Khosla C., *Appl. Environ. Microbiol.* **2002**, 68, 7, 3287-3292

20)Duckworth H.E.; Barber R.C.; Venkatasubramanian V.S. *Mass Spectroscopy*; 2nd ed.; Cambridge University Press: Cambridge, 1990.

21)Thomson J.J. *Phil. Mag.* **1912**, *24*, 668.

22)Aston F.W. *Phil. Mag.* **1919**, *38*, 709.

23)Aston F.W. *Phil. Mag.* **1920**, *39*, 449-445.

24)Aston F.W. *Phil. Mag.* **1923**, *45*, 934-945.

25)Dempster A.J. *Phys. Rev.* **1918**, *11*, 316.

26)Nier A.O.C. *Review of Scientific Instruments* **1947**, *18*, 398.

27)Williams D.H.; Fleming I. *Spectroscopic Methods in Organic Chemistry*; 4th ed.; McGraw Hill Book Company (UK) Limited: London, 1987.

28)Munson B. *Anal. Chem.* **1971**, *43*, A28.

29)Munson M.S.B.; Field F.H. *J. Am. Chem. Soc.* **1962**, *88*, 1621.

30)Macfarlane R. D. *Acc. Chem. Res.* **1982**, *15*, 268.

31)McNeal C. *Anal. Chem.* **1982**, *54*, 43A.

32)Dole M.; Mack L.L.; Hines R.L.; Mobley R.C.; Ferguson L.D.; Alice M.B. *J. Chem. Phys.* **1968**, *49*, 2240-2249.

33)Mack L.L.; Kralik P.; Rheude A.; Dole M. *J. Chem. Phys.* **1970**, *52*, 4977-4986.

34)Yamashita M.; Fenn J.B. *J. Phys. Chem.* **1984**, *88*, 4451-4459.

35)Yamashita M.; Fenn J.B. *J. Phys. Chem.* **1984**, *88*, 4671-4675.

36)Yates III, J. R. *J. Mass Spectrom.* **1998**, *33*, 1-19.

37)Loo J.A.; Edmonds C.G.; Smith R.D. *Science* **1990**, *248*, 201-204.

38)Fenn J.B.; Mann M.; Meng C.K.; Wong S.F.; Whitehouse C.M. *Mass Spec. Rev.* **1990**, *9*, 37-70.

39)Cole R.B. *Electrospray Ionisation Mass Spectrometry, Fundamentals, Instrumentation and Applications*; 1st ed.; John Wiley and Sons, INC., 1997.

40)Thomson B. A.; Iribarne J.V. *J. Chem. Phys.* **1979**, *71*, 4451.

41)Iribarne J.V.; Thomson B.A. *J. Chem. Phys.* **1976**, *64*, 2287.

42)Fenn J. B. *J. Am. Soc. Mass Spectrom.* **1993**, *4*, 524-535.

43)Benyon J. H.; Brenton A. G. *An Introduction to Mass Spectrometry*; 1st ed.; University of Wales Press: Cardiff, 1982.

44)Paul W.; Steinwedel H. *Zeitschrift fur Naturforschung* **1953**, *8a*, 448.

45)Paul W.; Reinhard.; von Zahn U. *Zeitschrift fur Physik* **1958**, *152*, 143.

46)Stephens W. E. *Phys. Rev.* **1946**, *69*, 691.

47)Cameron A. E.; Eggers D.F. *Review of Scientific Instruments* **1948**, *19*, 605.

48)Mirgorodskaya O.A.; Shevchenco A.A.; Chernushevich I. V.; Dodonov A. F.; Miroshnikov A. I. *Anal. Chem.* **1994**, *66*, 99.

49)Stafford Jr G.C.; Kelly P.E.; Syka J. E. P.; Reynolds W.E; Todd J. F. J. *Int. J. Mass Spectrom. Ion Processes* **1984**, *60*, 85.

50)Glish G.; McLuckey S. A. *Int. J. Mass Spectrom. Ion Processes* **1991**, *106*, 1-20.

51)March R.E.; Todd J.F.J. *Practical Aspects of Ion Trap Mass Spectrometry, Volume 1*; 1st ed.; T., C., Ed.; CRC Press, 1995; Vol. 1.

52)Stafford Jr G. C.; Taylor D. M.; Bradshaw S. C.; Syka J. E. P. : *Proceedings of the 35th ASMS Conference on Mass Spectrometry and Allied Topics*, Denver, CO, 1987, pp 775.

53)Louris J. N.; Cooks R. G.; Syka J. E. P.; Kelly P. E.; Stafford Jr. G. C.; Todd J. F. J. *Anal. Chem.* **1987**, *59*, 1677.

54)Jonscher K.R.; Yates III J.R. *Anal. Biochem.* **1997**, *244*, 1-15.

55)Johnson J. V.; Yost R. A.; Kelley P. E.; Bradford D. C. *Anal. Chem.* **1990**, *62*, 2162.

56)McLuckey S.A.; Glish G.L.; Van Berkel G.J. *Int. J. Mass Spectrom. Ion Processes* **1991**, *106*, 213-235.

57)Brodbelt J. S.; Kenttamaa H. I.; Cooks R. G. *Org. Mass Spectrom.* **1988**, *23*, 6.

58)Penning F. M. *Physica* **1936**, *3*, 873.

59)Comisarow M. B.; Marshall A. G. *Chem. Phys. Lett.* **1974**, *25*, 282-283.

60)Gauthier J. W.; Trantman T. R.; Jacobson D. B. *Anal. Chim. Acta* **1991**, *246*, 211-225.

61)McLafferty F. W. *Interpretation of Mass Spectra*; 2nd ed.; Benjamin Addison-Wesley: Massachusetts, 1973.

62)McLafferty F. W. *Org. Mass Spectrom.* **1980**, *15*, 114-121.

63)Maleknia S.; Brodbelt J. *Rapid Commun. Mass Spectrom.* **1992**, *6*, 376-381.

64)Gross M. L. *Int. J. Mass Spectrom. Ion Processes* **1992**, *118/119*, 137-165.

65)Cordero M. M.; Wesdemiotis C. *Anal. Chem.* **1994**, *66*, 861-866.

66)Wysocki V. H.; Ross M. M. *Int. J. Mass Spectrom. Ion Processes* **1991**, *104*, 179-211.

67)Delepine B.; Hurtaud-Pessel D.; Sanders P. *J. AOAC Int.* **1996**, *79*, 397-404.

68)Williams D. H. *Acc. Chem. Res.* **1977**, *10*, 280.

69)Weeks D. P.; Field F. H. *J. Am. Chem. Soc.* **1970**, *92*, 1600.

70)Bauerle G. F.; Brodbelt J. S. *J. Am. Soc. Mass Spectrom.* **1995**, *6*, 627-633.

71)Bigler L.; Hesse M. *J. Am. Soc. Mass Spectrom.* **1995**, *6*, 634-637.

72)Weissman K. J.; Kearney G. C.; Leadlay P. F.; Staunton J. *Rapid Commun. Mass Spectrom.* **1999**, *13*, 2103-2108.

73)Ward R. S.; Williams D. H. *J. Org. Chem.* **1969**, *34*, 3373.

74)Turecek F.; Smutek M.; Hanus V. *Org. Mass Spec.* **1981**, *16*, 483.

75)Sack T. M.; Lapp R. L.; Gross M. L. *Int. J. Mass Spectrom. Ion Processes* **1984**, *61*, 191-213.

76)Gates P. J.; Kearney G. C.; Jones R.; Leadlay P. F.; Staunton J. *Rapid Commun. Mass Spectrom.* **1999**, *13*, 242-246.

77)Hopfgartner G.; Chernushevich I. V.; Covey T.; Plomley J. B.; Bonner R. *J. Am. Soc. Mass Spectrom.* **1999**, *10*, 1305-1314.

78)Flora J. W.; Hannis J. C.; Muddiman D. C. *Anal. Chem.* **2001**, *73(6)*, 1247-1251

79)Kearney G. C.; Khan T.; Castro-Perez J.; Pugh J. *Proceedings of the 49th ASMS Conference on Mass Spectrometry and Allied Topics, Chicago, Illinois,* **2001**.

80)Gharbi-Benarous J.; Delaforge M.; Jankowski C.K.; Girault J.P. *J. Med. Chem.* **1991**, *34*, 1117-1125.

81)Gates P. J. *PhD Thesis*; University of Cambridge: Cambridge, 1999.

82)Alam P.; Buxton P.C.; Parkinson J.A.; Barber J. *J. Chem. Soc., Perkin Trans. 2* **1995**, 1163-1167.

83)Brull L. P.; Kovacik J. E.; Thomas-Oates J. E.; Heerma W.; Haverkamp J. *Rapid Commun. Mass Spectrom.* **1998**, *12*, 1520-1532.